

Cepheids and Long Period Variables in NGC 4395

F. Thim^{1,3}

National Optical Astronomy Observatory
950 North Cherry Ave., Tucson, AZ 85726

thim@noao.edu

J. G. Hoessel^{2,3}

Washburn Observatory, University of Wisconsin-Madison, 475 N. Charter Street, Madison,
Wisconsin 53706

hoessel@astro.wisc.edu

A. Saha^{1,2,3}, J. Claver^{1,3}, A. Dolphin^{1,3}

National Optical Astronomy Observatory
950 North Cherry Ave., Tucson, AZ 85726

saha@noao.edu, jclaver@noao.edu, dolphin@noao.edu

and

G. A. Tammann^{1,3}

Astronomisches Institut der Universität Basel
Venusstrasse 7, CH-4102 Binningen, Switzerland

G-A.Tammann@unibas.ch

Received _____; accepted _____

¹NOAO is operated by the Association of Universities for Research in Astronomy, Inc. (AURA) under cooperative agreement with the National Science Foundation.

²Visiting Astronomer, Kitt Peak National Observatory, National Optical Astronomy Observatory, which is operated by the Association of Universities for Research in Astronomy, Inc. (AURA) under cooperative agreement with the National Science Foundation.

³The WIYN Observatory is a joint facility of the University of Wisconsin-Madison, Indiana University, Yale University, and the National Optical Astronomy Observatory.

ABSTRACT

Repeated imaging observations of NGC 4395 were made with the WIYN 3.5 m and the KPNO 2.1 m telescopes. From the photometry of the resolved brighter stars in this galaxy eleven Cepheids with periods ranging between 12 and 90 days have been identified. The true distance modulus has been derived from the apparent distance moduli in g , r and i . The distance modulus is 28.02 ± 0.18 based on the LMC P-L relation by Sandage, Reindl & Tammann (2003); this corresponds to a distance of 4.0 ± 0.3 Mpc. Using the P-L relation from Madore & Freedman (1991), the distance modulus is 28.15 ± 0.18 ; which corresponds to a distance of 4.3 ± 0.4 Mpc. The reddening is calculated to be $E(g - r) = 0.06 \pm 0.08$ and $E(r - i) = 0.10 \pm 0.08$, again from the distance moduli μ_g , μ_r and μ_i . In addition, 37 other variables have been detected, the majority of which have definite periods. They are probably all red long period variables.

Subject headings: Cepheids — Stars: variables: other — distance scale — galaxies: individual (NGC 4395)

1. Introduction

NGC 4395 ($\alpha_{2000}=12^{\text{h}}25^{\text{m}}48.92^{\text{s}}$, $\delta = +33^{\circ}32^{\text{m}}48.3^{\text{s}}$) is a face-on spiral galaxy that is classified as Sd III-IV in the Carnegie Atlas of Galaxies (Sandage & Bedke 1994). It is located in the Ursa Major region called Group B4 by Kraan-Korteweg & Tammann (1979) and CVn I by de Vaucouleurs (1975).

NGC 4395 is a pure disk galaxy, i.e. it lacks a bulge (Filippenko & Ho 2003). It is also the nearest known Seyfert 1 galaxy and has a central black hole for which the total mass has recently been derived by Filippenko & Ho (2003). They estimate the mass of the

central black hole to be $\sim 10^4 - 10^5 M_{\odot}$, which is less massive than those which have been found in other AGNs. All other galaxies with known supermassive black holes in their centers have bulges, which makes NGC 4395 a unique object.

Literature distance estimates range between 2.6 Mpc (Rowan-Robinson 1985) and 5.0 Mpc (Sandage & Bedke 1994). More recently, Karachentsev & Drozdovsky (1998) estimated the distance to NGC 4395 to be 4.2 ± 0.8 Mpc using the brightest blue stars. Hubble Space Telescope/WFPC2 images have been used by two groups for the distance estimate, Karachentsev et al. (2003) obtained a tip of the red giant branch (TRGB) distance of 4.61 ± 0.57 Mpc, Minitti et al. (2003) derived a distance of 4.2 Mpc.

Repeated time spaced images of NGC 4395 were obtained as part of a program begun by Saha & Hoessel in 1990 to determine Cepheid distances to several galaxies in the Local Group as well as beyond. The project was motivated in part by the desire to extend the range of ground based Cepheid distances by employing the technological advantage of CCDs. While the *Hubble Space Telescope* would surely vastly extend this range, we proceeded on the premise that relatively nearby objects which can be reached from the ground would not, and should not, occupy the precious and expensive resources of the *HST*. Nevertheless, the cartography of the local Universe continued to be an important problem.

Ground based time-sequence observations are inevitably impeded by constraints from telescope scheduling, weather and poor seeing. As a result, some of the objects (particularly the more distant and more demanding ones) selected in our initial program with the Kitt Peak 2.1-m telescope could not be completed. With the commissioning of the WIYN 3.5-m telescope (also on Kitt Peak) we got not only an increase in aperture, but also better image quality. Additionally, and very important, for a time while the NOAO queue observations were being conducted regularly, the necessary observations for the unfinished galaxies could be obtained efficiently.

While the time span to obtain the observations for the Cepheid discovery in NGC 4395 took a frustrating 8 years, a side benefit is that many long period variables (LPVs) were also discovered, for which periods could be determined. The literature lacks period, luminosity and color information for LPVs, except in a very few galaxies (the Magellanic Clouds, M33), and consequently the empirical properties of LPVs and their dependence on metallicity (for instance) are very poorly known. We hope that the LPVs we have been able to catalog here for NGC 4395 is a step towards ameliorating this situation.

2. Observations

Images of NGC 4395 were taken using two different telescopes, the WIYN 3.5 m telescope, and the 2.1 m KPNO telescope, which are both located on Kitt Peak. These repeated images were obtained over a period of 8 years, from 1991 January 13, to 1999 January 13 in the g , r and i passbands of the Thuan & Gunn (1976) system.

The detectors which have been used are named TI-2, TIKA and S2KB. TI-2, used on the 2.1 m, is a 796×796 CCD with a pixel size of $15 \mu\text{m}$ and a scale of $0''.2/\text{pixel}$. T1KA, also used on the 2.1 m, is a 1024×1024 CCD which provides a pixel scale of $0''.305/\text{pixel}$ and a field of view of $5''.2 \times 5''.2$. S2KB was exclusively for the WIYN telescope, it is a 2048×2048 CCD with $21 \mu\text{m}$ pixels. This provides a pixel scale of $0''.197/\text{pixel}$ and a field of view of $6''.8 \times 6''.8$. The exposure times are between 500 and 1200 s. A journal of the observations is given in Table 1.

Primary observations were in the r -band, which was optimal for the color response of the early CCDs used, given both, the color range of Cepheids, and the region of the spectrum where the sky is sufficiently dark. Supplemental observations were made at four epochs in the g band and at two epochs in the i band, so that mean colors for the Cepheids

could be derived, and used to track extinction and reddening.

3. Data Processing

3.1. Relative Photometry and Object Matching

Multiple exposures obtained with WIYN S2KB were combined and used as a template fits file. The reference image in r is shown in Fig. 1. This image is also provided as a FITS file in the electronic version of this paper. Positions (X and Y in pixels) of objects given in various tables in this paper can be easily located on the electronic image. The published FITS image is also appointed with a ‘world coordinate system’ (WCS) calibrated to J2000 coordinates on the sky.

The reference image is used as a position reference only. For visualization and ‘blinking’ of images, the individual epoch images were mapped to the reference image. However, photometry (see below) for the individual epochs was always done on the untransformed original images, so that noise characteristics on the image remain untainted, and also to avoid the seeing degradation from the transformation.

Relative photometry and object identification on the template images were obtained with the program DoPHOT (Schechter, Mateo, & Saha 1993). Subsequently DoPHOT was run on each individual epoch. All objects identified in the individual epochs were matched to the template frame and the coordinate transformations for the individual epochs were derived. The relative photometry at each epoch differs from that in the template frame by a constant magnitude offset. This offset is easily determined from the ensemble average of the difference between matched stars in the template and the epoch. In order to avoid issues with bias at faint magnitudes, as well as with bad outliers, this procedure is best done by inspecting a plot of the magnitude difference for each star versus the magnitude on

the template image. This puts the relative magnitudes of all stars in all epochs in r on the same footing. A similar procedure was used for the g and i passbands as well. In practice, the template magnitudes in the 3 bands had already been adjusted to the true Thuan-Gunn system using the procedure described in the following sub-section, so the final magnitudes for each epoch were also on the Thuan-Gunn system.

3.2. Calibrating the Photometry

Additional observations of NGC 4395 along with observations of standard stars were taken with the S2KB detector on the WIYN 3.5m telescope in the Thuan-Gunn g , r , i bands on 2000 May 26 (UT date). The images of NGC 4395 taken on this night were shallower exposures to ensure that some of the brighter isolated stars would not be saturated. A photometric solution was obtained for that night from the standard star observations. The error in the mean for the primary standard stars on this night is less than 0.01 mag in all three passbands.

Aperture photometry of several bright and relatively uncrowded stars in the field of NGC 4395 were obtained, and true magnitudes derived using the photometric solution for that night. Sky subtraction in all cases was done using the ‘growth curve’ method. Thus local standards in g , r , and i were established in the field of NGC 4395. These local standards are identified by the letters A, B, C, D and Z, and are shown in Fig. 1. Their magnitudes are listed in Table 2 along with their X and Y positions on the template image, and also their coordinates on the sky. The standard error of measurement for each star is less than 0.015 mag rms. In addition, 3 relatively fainter stars were also calibrated as local standards, but using PSF fitting and aperture correction. These stars are designated as $f1$, $f2$, and $f3$, and are also shown in Fig. 1 with magnitudes listed in Table 2. For these 3 fainter objects, the standard error is ~ 0.03 mag rms per star. A conservative estimate

is that the magnitude scales and colors are calibrated to within a systematic error not exceeding 0.05 mag.

Armed with this calibration, the relative photometry described in the preceding section is adjusted to the true Thuan-Gunn system by comparing the relative photometry of an ensemble of several thousand stars from any epoch or template with stars found in common on the images taken on the calibrating night.

4. Identification of the Variable Stars

4.1. Detection of Variable Stars

Given photometry and photometric errors in all epochs, each object was examined for variability. The method for identifying variable stars is described in Saha & Hoessel (1990) and is not repeated here. The requirements for variability have been improved since Saha & Hoessel (1990) from experience with similar data. The individual magnitudes measured in the various epochs and their individual errors estimates for each of the Cepheids in g , r and i are tabulated in Table 3, the individual magnitudes and errors of the other variable stars in g , r and i are tabulated in Table 4.

If P is the period of a supposed variable star, m_i the measured magnitude at the i th epoch, and \bar{m} the average over the n values of m_i , and if the values for m_i are arranged in increasing order of phase, then Θ is defined as:

$$\Theta(P) = \frac{\sum_{i=1}^n (m_{i+1} - m_i)^2}{\sum_{i=1}^n (m_i - \bar{m})^2}. \quad (1)$$

A minimum in the spectrum of Θ indicates a possible period. The reduced χ^2 is given by:

$$\chi_\nu^2 = \sum_i^n \frac{(m_i - \bar{m})^2}{\nu \sigma_i^2}, \quad (2)$$

where σ_i is the rms error and $\nu = n - 1$. Λ (Lafler & Kinman 1965; Saha & Hoessel 1990) is related to Θ in the sense that Λ goes as $\frac{1}{\Theta}$. An object is considered to be variable if the χ^2 probability is higher than 0.99 and Λ greater than 3.5. Furthermore, an object with a reduced χ^2 higher than 100 is always flagged to be a possible variable. The requirements and changes from Saha & Hoessel (1990) are described in more detail in Saha, Claver, & Hoessel (2002).

Sixty four out of a total of 25,155 stars in the template r frame are flagged to be possible variables. These candidates are examined for periodicity using the method of Lafler & Kinman (1965). The period range from 1 to 3000 days has been used to probe possible variability. Only data in the r band have been used for the variable search because only 4 epochs in the g and 2 in the i band have been taken, which is insufficient to derive a period. The objects which are likely to be Cepheids are presented in Table 5, the remaining other variables are listed in Table 6. As a double check on the variability all candidates have been visually blinked and compared with non-variable stars. The periods are given in column 2. The periods for some variables in Table 6 are uncertain, with uncertainties ranging from a few days to a few hundred days. In such cases, we present our best guess in the table.

The mean magnitudes in r are phase-weighted intensity averaged means and were calculated using the following equation:

$$\langle r \rangle = -2.5 \log_{10} \sum_{i=1}^n 0.5 (\phi_{i+1} - \phi_{i-1}) 10^{-0.4r_i}, \quad (3)$$

where n is the number of observations, r_i the magnitude, and ϕ_i the phase of the i th observation in order of increasing phase. Intensity weighted magnitudes can be biased due to missing measurements, – biased in a sense that it is more likely to detect the variable star at a brighter than at a fainter phase. The phase-weighted intensity mean gives isolated points more weight than closely spaced ones, which makes it superior to a straight intensity mean. The method to use well-sampled lightcurves to predict corrections to small samplings

at another wavelength in order to predict their mean magnitudes originates with Freedman (1988). We are using here a similar method described in Labhardt, Sandage, & Tammann (1997). The mean g magnitudes in Table 5 are calculated using the information on the shape and the amplitude of the complete light curve in one filter as well as the typical phase shift between two filters are used to derive a value of $\langle g \rangle$ from each g measurement. Labhardt et al. (1997) presents transformations for the filters B, V, R and I. Therefore, the empirical correction function between V and R have been transformed to g and r using synthetic transformations and amplitude ratios.

4.2. Identification of Cepheid Variables and Period Determination

The light curves of all possible variable stars with reasonable values of Θ were individually inspected by eye in all three passbands. However, in g and i there have been sometimes only one or even zero photometric measurements, which makes the term “light curve” meaningless. In such cases, the color estimate is rather uncertain. The light curves of the Cepheid candidates are shown in Fig. 2.

The quality of the light curve in r , the quality of the light curve in g , the phase coherence between the r , the g and i light curves, the shape of the spectrum of Θ and the $g - r$ and $r - i$ colors have been used as the selection criteria to consider a variable star being a Cepheid or not.

Since there are very few epochs with measurements in the g band, the mean $\langle g \rangle$ magnitudes are calculated using the method of Labhardt et al. (1997), with an equation of the form:

$$\langle g \rangle = g(\phi_r) + [\langle r \rangle - r(\phi_r)] + \Delta r C_{r \rightarrow g}(\phi), \quad (4)$$

where Δr is the r amplitude, $\langle r \rangle$ the phase-weighted mean r magnitude, ϕ the phase of

the light curve and $C_{r \rightarrow g}(\phi)$ the empirical function for the transformation between r and g magnitudes. Labhardt et al. (1997) listed values of $C(\phi)$ for B, V, R, I mags, from which we can derive $C_{r \rightarrow g}(\phi)$, using the equation:

$$C_{r \rightarrow g}(\phi) = 1.722C_{V \rightarrow R}(\phi) + 0.655C_{V \rightarrow B}(\phi), \quad (5)$$

$C_{V \rightarrow R}(\phi)$ are the correction values for $V \rightarrow R$ magnitudes, $C_{V \rightarrow B}(\phi)$ the value for $V \rightarrow B$ magnitudes, and are listed in Labhardt et al. (1997). The derivation of the above equation uses color transformations that are discussed in § 5.

The mean of the individual $\langle g \rangle$ magnitudes yields the adopted value of $\langle g \rangle$ and its error. The i magnitudes are calculated from the $r - i$ color at the i phase and the mean $\langle r \rangle$ values, (i.e. setting $C_{r \rightarrow i}(\phi)$ to zero).

In total, we identified 11 Cepheids, which are listed in Table 5. Column 1 gives the designation of the Cepheid, column 2 the period, columns 3-8 give the mean magnitudes and errors in g , r , and i , and columns 9-10 their position on the template r image.

As noted before, all variable stars have been visually blinked. Nine of the eleven Cepheids in Table 5 blink, whereas it is hard to tell for the Cepheids C4 and C11 because of their small amplitudes. Besides these eleven candidates no further Cepheid candidates have been accepted.

4.3. Long Period Variables

The remaining candidates, which have not been classified as Cepheid variables, are listed in Table 6. We found 37 variables besides the 11 Cepheids. Again, column 1 gives the designation of the variable, column 2 the period, columns 3-5 give the mean magnitudes in g , r , and i , column 6 the r peak to peak amplitude, and columns 7-8 their position on the template r image. The r amplitude is estimated from the peak to peak magnitude from

their smoothed light curves rather than from the difference of minimum and maximum measured magnitudes. All variables have been visually inspected by blinking pairs of images in order to see variability, i.e. images near maximum brightness were compared against images near minimum brightness. All candidates in Table 6 are varying intrinsically in brightness. 16 of these variables have an uncertain period; in these cases the best guess for the period estimate is presented. Their light curves are presented in Fig. 3.

The variables in Fig. 6 have $g - r$ colors between 0.5 and 1.6 and $r - i$ colors of about 0.2 to 1.2, which indicates that these variables are red giants. No Luminous Blue Variable (LBVs), or Hubble-Sandage Variable (Hubble & Sandage 1953) has been identified. A detailed discussion of the LPVs is taken up in §7.2 later in the paper after we have derived the distance modulus.

5. The Cepheid Period-Luminosity Relation

5.1. The Period-Luminosity Relation using the Kent Transformations

The transformation equations from the Johnson to the Thuan-Gunn filter system given by Kent (1985) are:

$$V = g - 0.03 - 0.42 (g - r) \quad (6)$$

$$R = r - 0.51 - 0.15 (g - r). \quad (7)$$

For the i band the Wade et al. (1979) transformations have been used. These transformations which are valid for a color range which are typical for Cepheids are given by:

$$i = 0.999I + 0.690 + 0.419 (R - I). \quad (8)$$

The P-L relation in $BVRI$ from Madore & Freedman (1991), can be transformed using

the relations by Kent (1985) and Wade et al. (1979) to be:

$$M_g = -2.62(\log P - 1) - 4.08 , \quad (9)$$

$$M_r = -2.91(\log P - 1) - 4.04 , \quad (10)$$

$$M_i = -3.00(\log P - 1) - 4.06 , \quad (11)$$

as derived in Hoessel et al. (1994).

5.2. The Period-Luminosity Relation using Synthetic Transformations

Transformations that better reflect the spectral energy distribution (SED's) of supergiants with temperatures spanning that of Cepheids can be obtained synthetically.

The observed SED's of several Thuan-Gunn standard stars spanning a wide range of color integrated for model bandpasses of g , r and i . The transformation to convert the resulting 'instrumental' magnitudes to true magnitudes on the Thuan-Gunn system was derived.

The same was done for the $BVRI$ Johnson-Cousins-Landolt system.

Once we were able to accurately reproduce the stellar photometry from the stellar spectra, we computed synthetic magnitudes in both filter systems – Johnson-Cousins-Landolt and Thuan-Gunn – from synthetic stellar spectra (Kurucz). Limiting this work to stars with temperatures and gravities within and slightly beyond the range of Cepheids, we computed the following transformations from the Johnson-Cousins-Landolt system to the Thuan-Gunn system:

$$g - V = -0.102 + 0.393(B - V) \quad (12)$$

$$r - R = 0.437 - 0.033(V - R) \quad (13)$$

$$i - I = 0.816 - 0.081(R - I). \quad (14)$$

Because these transformations were computed over a limited range of temperature, gravity, and metallicity, no second-order color terms are necessary. Naturally, this also means that these transformations are useful only for stars in this restricted range of parameters. Because the range in color of the Cepheids under consideration is quite limited, the linear approximation in eq. 12-14 is sufficient.

Applying these synthetic transformations to the P-L relations of Madore & Freedman (1991) leads to the P-L relations in the Gunn system:

$$M_g = -2.63(\log P - 1) - 4.00, \quad (15)$$

$$M_r = -2.95(\log P - 1) - 4.09, \quad (16)$$

$$M_i = -3.07(\log P - 1) - 4.08. \quad (17)$$

Eq. 16 – 17 (r and i bands) compare favorably with their counterparts (equations 10 and 11) from Hoessl et al. (1994) based on the Kent (1985) transformations. But in the g band (eq. 15 compared to eq. 9) the difference is quite significant. The effect in terms of measured apparent distance moduli is:

$$\delta \mu_g = 0.01(\log P - 1) - 0.08 \quad (18)$$

$$\delta \mu_r = 0.04(\log P - 1) + 0.05 \quad (19)$$

$$\delta \mu_i = 0.07(\log P - 1) + 0.02, \quad (20)$$

where the sign is distance modulus from eq. 15 – 17 minus Hoessel et al. (1994). For a Cepheid with a period of 25 days, the differences are -0.08 magnitudes in g , $+0.07$ magnitudes in r , and $+0.04$ magnitudes in i . The synthetic transformations are superior to the older ones, since they are based on empirical observations of stars which are mostly dwarfs, and whose SEDs differ systematically from supergiants. Our previous studies were based on ri photometry, and thus the color errors were small enough to be unnoticeable – but here, when the g band is used, the synthetic transformations are necessary, particularly since we will see in § 6 that the Kent transformations imply reddening values that are inconsistent with the observed colors of the bluest stars in NGC 4395.

The observed P-L relations are shown in Fig. 4 for the g and the r bands. Since the slope is fixed, the remaining free parameter is the offset which corresponds to the apparent distance moduli in g and r . The dashed lines indicate the intrinsic width of the P-L relation. The reported uncertainties are the standard errors, i.e. the rms scatter divided by the square root of the number of Cepheids.

6. Extinction and the Distance Modulus

In order to derive the absorption-reddening relations

$$R_{g,r} = \frac{A_{g,r}}{E(g - r)}, \quad (21)$$

we have synthesized ' g ' and ' r ' magnitudes for Cepheid spectra as in section 5.2, but now additionally including extinction using the equations of Cardelli, Clayton, & Mathis (1989). We adjusted the value of R_V to be that for which $A_V/E(B - V)$ is 3.1.

By comparing the results from different amounts of input absorption, we derived $A_g/E(g - r) = 3.44$. The true distance modulus is then given by

$$\mu_0 = \mu_g - A(g) = 3.44\mu_r - 2.44\mu_g. \quad (22)$$

(cf. Tamman, Sandage, & Reindl 2003, eq. 40.)

We have applied the transformed P-L_{*g,r*} relations in eq. 15 and 16, which are based on the old P-L_{*B,V,R*} relations by Madore & Freedman (1991), to the 11 Cepheids in NGC 4395. The resulting apparent distance moduli μ_g and μ_r are shown for each star in Table 7 as well as the individual true distance moduli from eq. 22. The mean true distance modulus of NGC 4395 is then found to be

$$\mu_0 = 28.22 \pm 0.21. \quad (23)$$

The apparent moduli μ_g and μ_r in Table 7 imply a mean reddening of the Cepheids of $E(g-r) = 0.059$.

If we use the P-L relation of Madore & Freedman (1991) with transformations by Kent (1985) the true distance modulus μ_0 would be 27.80 with a large reddening $E(g-r)$ of 0.20 (see Table 7). An examination of our CMD (Fig. 6) indicates that the bluest stars are too blue to have a reddening of $E(g-r)=0.20$, as the blue edge of the CMD is roughly 0.1 magnitudes redward of the theoretical limit of $g-r=-0.8$, which therefore means that $E(g-r)$ cannot be > 0.1 . This convinces us that the P-L relations from the synthetic transformations are more accurate and we adopt them in this paper.

The true distance modulus to NGC 4395 and the reddening can also be obtained with the mean *r* and *i* magnitudes of the Cepheids. The individual mean magnitudes are listed in Table 5. As shown in Table 3, the number of observations in the *i* band is 1 or 2, except C08, which has no *i* magnitude. The mean *i* magnitude is calculated from the *r-i* color at *i* phase. Using again the P-L relation of Madore & Freedman (1991) and the transformations by Kent (1985) for the *r* band and in addition the transformations by Wade et al. (1979)

for the i band, we obtain $\mu_i = 28.20 \pm 0.12$ and $E(r - i) = 0.09 \pm 0.08$. If we use the P-L relation of Madore & Freedman (1991) with the synthetic transformations the mean μ_i is calculated to be 28.26 ± 0.13 with a mean $E(r - i)$ reddening of 0.10 ± 0.09 . The individual values are presented in Table 8. The true distance modulus is given by

$$\mu_0 = 3.72 \mu_i - 2.72 \mu_r \quad (24)$$

(Saha et al. 2002, eq. 10), which leads to $\mu_0 = 27.96 \pm 0.34$ and 27.98 ± 0.34 for the Kent and Wade and the synthetic transformations, respectively. This agreement demonstrates that use of the Kent-Wade transformations for r and i used in previous papers is consistent with the new synthetic relations. The estimated error in the present case, from using r and i is much larger than that from using g and r because of the fewer i observations compared to g observations. In the following, we exclusively use the distances obtained with the synthetic transformations. We calculate the assumed true distance to NGC 4395 with the weighted mean of the true distances obtained with g and r on one hand, and the distance obtained with r and i on the other hand. The true weighted distance modulus is then given by combining both sets of distances:

$$\mu_0 = 28.15 \pm 0.18 \quad (25)$$

using the Madore & Freedman (1991) P-L relations.

The Galactic reddening of $E(g - r) < 0.02$ (Burstein & Heiles 1984; Schlegel, Finkbeiner, & Davis 1998) cannot account for the full reddening of the Cepheids. They must suffer additional reddening in the parent galaxy. The diagnostic diagram in Fig. 5 suggest that the intrinsic reddening is quite uniform.

A new fundamental problem with Cepheid distances arises from the fact that P-L relations in different galaxies are different (Tammann et al. 2002). The Galactic P-L relation is markedly steeper than in LMC, the latter being in addition non-linear (Tammann et al.

2003). The authors show that at least part of these differences are due to metallicity differences. If metallicity alone decides about the form of the P-L relation, NGC 4395 with $12 + \log \text{O/H} = 8.33 \pm 0.25$ (Roy et al. 1996) is similar to LMC and should be compared with the LMC P-L relation. The latter has been derived by Sandage et al. (2003) from the vast data by Udalski et al. (1999) which are augmented from external sources for longer-period Cepheids. The new LMC P-L relations for Cepheids with periods more than 10 days in V and I are given by

$$M_V = -(2.609 \pm 0.099) \log P - (1.565 \pm 0.131), \quad (26)$$

$$M_I = -(2.864 \pm 0.082) \log P - (2.010 \pm 0.108). \quad (27)$$

Therefore, the true final dereddened distance modulus becomes

$$\mu_0 = 28.02 \pm 0.18. \quad (28)$$

We prefer this value over $\mu_0 = 28.26 \pm 0.18$ which one would obtain from the P-L relation of the Galaxy, which is clearly more metal-rich than NGC 4395.

7. The Color-Magnitude Diagram, Extinction Estimates and LPVs

7.1. The Color-Magnitude Diagram and Extinction Estimates

The color-magnitude diagrams for the template frames for g , r and r , i are shown in Fig. 6 and 7. The large filled circles mark the position of the mean magnitudes of the Cepheids, open large circles indicate the position of the mean magnitudes of all other variable stars. The position of the Cepheids in the CMDs is consistent with expectation. The majority of other variables have red colors and periods longer than hundreds of days. They are listed in Table 6, their light curves are presented in Fig. 3.

As stated before, an examination of our CMD indicates that the bluest stars are too blue to have a reddening of $E(g - r) = 0.20$, as the blue edge of the CMD is roughly 0.1 magnitudes redward of the theoretical limit of $g - r = -0.8$. Thus we believe the P-L relations from the synthetic transformations to be more accurate and adopt them in this paper.

7.2. The Long Period Variables

Kholopov et al. (1985) defined three types of variable red giant stars. First, the Mira type variables are long period variables with periods in the range between 80 and 1000 days and amplitudes in the V band between 2.5 and 11 mag. Second, the semiregular variables which have smaller amplitudes, from several hundredths to 1-2 mag in the V band, their period range is between 20 to 2000 days or more and their light curves show a less regular behavior. The third group of variables are the irregular variables having amplitudes of the order of 1 mag in the V band. Kholopov et al. (1985) also mention that many stars are mis-classified as irregular variables because of incomplete studies.

The Kholopov et al. (1985) classification is based in the main on stars observed within our Galaxy. The selection effects for Galactic variable stars is very different from that for external galaxies. Within our Galaxy, fainter relatively nearby variables abound, whereas very luminous variables, which are also short lived, are relatively rare, and since they occur in the disk, are often obscured behind a lot of dust. On the other hand, in external galaxies, these are much more easily seen, since they are among the brightest stars. In a near face-on case like in NGC4395, extinction and obscuration are less significant. A better template for comparing the LPVs is from the sample from the Kinman, Mould, & Wood (1987) study in M33. In their analysis, Kinman et al. (1987) identified red long period variables (LPVs) as either core-helium-burning as or as upper asymptotic giant branch

(AGB) stars. Core-helium-burning, or red supergiant (RSG) stars are at least 1 magnitude brighter than AGB stars (Wood, Bessell, & Fox 1983). The RSG long period variables are seen to have smaller amplitudes than the AGB stars (Wood & Bessell 1985). In the r -band, typical amplitudes for RSG variables are a magnitude or smaller, whereas for the AGB LPVs amplitudes as large as 3 mags are quite common. Further, an AGB star has a degenerate core, and its luminosity is determined by its core mass, which in turn is subject to the Chandrasekhar limit. This implies an upper limit on the luminosity of an AGB star of $M_{bol} \approx -7.0$, which is equivalent to $M_r = -5.20$ mag (Kinman et al. 1987).

To see if the above characteristic criteria can be used to distinguish between AGB and RSG LPVs, consider Fig. 8, where the mean r magnitudes of all possible long period variables are plotted against their r amplitude. A clear break in the $\langle r \rangle$ magnitude distribution can be seen: there are four LPVs fainter than $\langle r \rangle = 23.2$ with the rest mostly brighter than $\langle r \rangle = 22$ mag. Anticipating (in §6) the apparent distance modulus in r of 28.36, we conclude that an AGB star can be no brighter than $r = 23.16$. We therefore argue that the four LPVs in Fig. 8 that are fainter than $r = 23.1$ are AGB stars, whereas the remainder are RSG LPVs. This argument is borne out by the location of these stars on the color-magnitude diagram obtained from our image data, as discussed in §7.1.

However, the amplitudes of these two ‘classes’ of LPVs do not follow expected behavior. The variables deduced to be AGB stars all have r amplitudes near 1.0 mag, which is smaller than typical. All but four of the putative RSG variables have reasonably small amplitudes, but the four with $\Delta r > 1.2$ mag clearly stand out in Fig. 8. This is not entirely without precedent, since Hoessel, Saha, & Danielson (1998) found three very high amplitude red variables in the dwarf galaxy DDO 187, where these stars are among the brightest stars in that galaxy. Hoessel et al. (1998) discussed the possibility that these were not the ‘usual’ RSG variables, but possibly the evolved products of Hubble-Sandage variables, with

pulsations driven by Kelvin-Helmholtz instabilities as predicted by Heger et al. (1997). In the case of the four objects in question here, V3, V15, V33 and V37, the amplitudes, while larger than expected for RSG LPVs, are much smaller than the three stars mentioned in DDO 187. Heger et al. (1997) expect periods near 900 days for the red descendants of Hubble-Sandage variables, if they are indeed driven by Kelvin-Helmholtz instabilities, as they predict, but this is not the case for the four stars at hand, which have periods from 210 to 820 days. We must stress that the *empirical* behavior of RSG LPVs is not known very well, and the moderately larger amplitudes for the four objects in discussion may not be so unusual after all. Only a systematic study of LPVs among young stellar populations with different metallicities can give us the answer.

8. Summary

We have presented the results of a search for variable stars in NGC 4395 using the WIYN 3.5 m and the KPNO 2.1 m telescopes. Since the observations have been accumulated over a time span of 8 years, we have been able to not only discover 11 Cepheids, but also 37 long period variables (LPVs). A true distance modulus of 28.02 ± 0.18 and a mean reddening $E(g - r)$ of 0.06 and of $E(r - i)$ of 0.10 have been derived from the apparent distance moduli in g , r and i based on the LMC P-L relation by Sandage et al. (2003). The de-reddened distance modulus corresponds to a distance of 4.0 ± 0.3 Mpc. This adds to the growing list of galaxies well outside the Local Group for which Cepheid distances are now obtained from ground based observations. NGC 4395 is of particular interest, since it is the nearest known Seyfert 1 galaxy.

Implying an upper limit on the luminosity of an AGB star of $M_r \approx -5.2$ (Kinman et al. 1987) and a distance modulus of 28.02, we concluded that 4 out of the 37 red long period variables are AGB stars, the rest probably being RSG LPVs.

Acknowledgments

The observations with the WIYN telescope were made in part through the queue-scheduled service observing program that was being run by NOAO. We thank Dianne Harmer, Paul Smith, and Daryl Willmarth for their participation in the observations.

REFERENCES

- Burstein, D. & Heiles, C. 1984, ApJS, 54, 33
- Cardelli, J.A., Clayton, G.C., & Mathis, J.S. 1989, ApJ, 345, 245
- de Vaucouleurs, G. 1975, Social Studies of Science, 9, 557
- Filippenko, A. V., & Ho, L. C. 2003, ApJ, 588, 13
- Freedman, W. L. 1988, ApJ, 326, 691
- Heger, A., Jeannin, L., Langer, N., & Baraffe, I. 1997, A&A 327, 224
- Hoessel, J. G., Saha, A., Krist, J., & Danielson, G. E. 1994, AJ, 108, 645
- Hoessel, J. G., Saha, A., & Danielson, G. E. 1998, AJ, 116, 1687
- Hubble, E. & Sandage, A. 1953, ApJ, 118, 353
- Karachentsev, I. D. & Drozdovsky, I. O. 1998, A&AS, 131, 1
- Karachentsev, I. D. et al. 2003, A&A, 398, 467
- Kent, S. M. 1985, PASP, 97, 165
- Kholopov, P. N., Samus, N. N., Frolov, M. S., et al. 1985-88, General Catalogue of Variable Stars. 4th edition, Nauka Publishing House, Moscow (GCVS)
- Kinman, T. D., Mould, J. R., & Wood, P. R. 1987, AJ, 93, 833
- Kraan-Korteweg, R.C., & Tammann, G.A. 1979, AN, 300, 181
- Kurucz, <http://kurucz.harvard.edu/>
- Labhardt, L., Sandage, A., & Tammann, G.A. 1997, A&A, 322, 751

- Lafler, J., & Kinman, T.D. 1965, ApJS, 11, 216
- Madore, B.F., & Freedman, W.L. 1991, PASP, 103, 933
- Minniti et al., 2003, in preparation
- Rowan-Robinson, M. 1985, New York, W. H. Freeman and Co, 1985, 364
- Roy, J., Belley, J., Dutil, Y., & Martin, P. 1996, ApJ, 460, 284
- Saha, A., & Hoessel, J.G. 1990, AJ, 99, 97
- Saha, A., Sandage, A., Labhardt, L., Tammann, G. A., Macchetto, F. D., & Panagia, N. 1996, ApJ, 466, 55
- Saha, A., Claver, J., & Hoessel, J. G. 2002, AJ, 124, 839
- Sandage, A. & Bedke, J. 1994, Washington, DC: Carnegie Institution of Washington with The Flintridge Foundation, —c1994
- Sandage, A., & Reindl, B., & Tammann, G.A. 2003, in preparation
- Schechter, P.L., Mateo, M.L., & Saha, A. 1993, PASP, 105, 1342
- Schlegel, D. J., Finkbeiner, D. P., & Davis, M. 1998, ApJ, 500, 525
- Tammann, G. A., Reindl, B., Thim, F., Saha, A., & Sandage, A. 2002, ASP Conf. Ser. 283: A New Era in Cosmology, 258
- Tammann, G. A., Sandage, A., & Reindl, B. 2003, A&A, 404, 423
- Thuan, T. X. & Gunn, J. E. 1976, PASP, 88, 543
- Udalski, A., Szymanski, M., Kubiak, M., Pietrzynski, G., Soszynski, I., Wozniak, P., & Zebrun, K. 1999, Acta Astronomica, 49, 201

Wade, R. A., Hoessel, J. G., Elias, J. H., & Huchra, J. P. 1979, PASP, 91, 35

Wood, P. R. & Bessell, M. S. 1985, PASP, 97, 681

Wood, P. R., Bessell, M. S., & Fox, M. W. 1983, ApJ, 272, 99

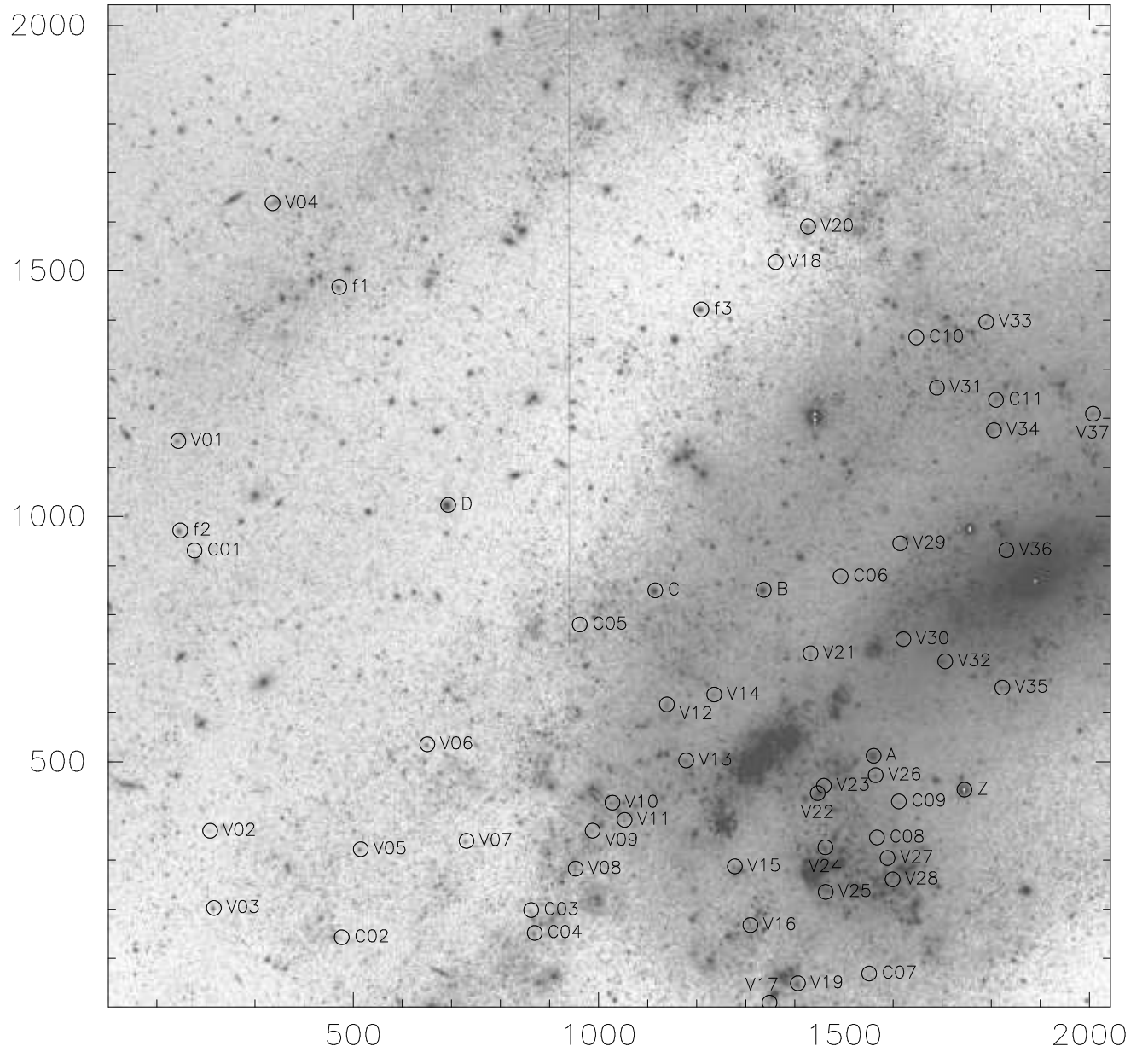


Fig. 1.— WIYN S2KB r image covering the field NE of the center of NGC 4395, which is located on the right side close to the edge of the chip. North is up and East is to the left. Cepheids and other long period variables are shown as open circles and labeled with C for Cepheids and V for other variables followed by a number. The labels are the same as given in Table 5 and 6. The local standards which are presented in Table 2 are also shown as open circles and are labeled by the letters A, B, C, D, Z, f_1 , f_2 , and f_3 .

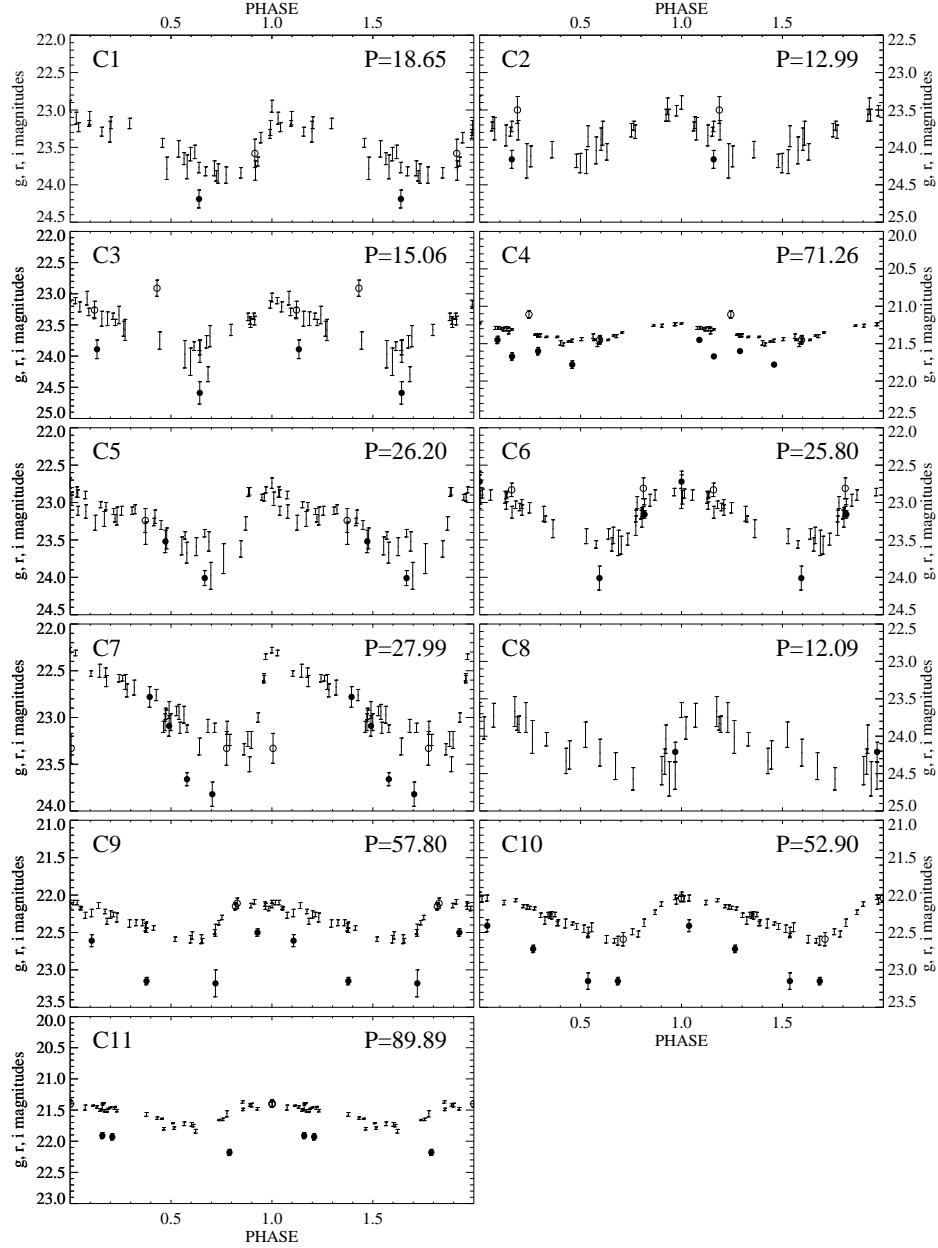


Fig. 2.— The light curves of the Cepheids in r (small dots with error bars), in g (large filled circles) and in i (large open circles). The identification numbers (C1-C11) and its periods are displayed in each graph. The periods are given in days.

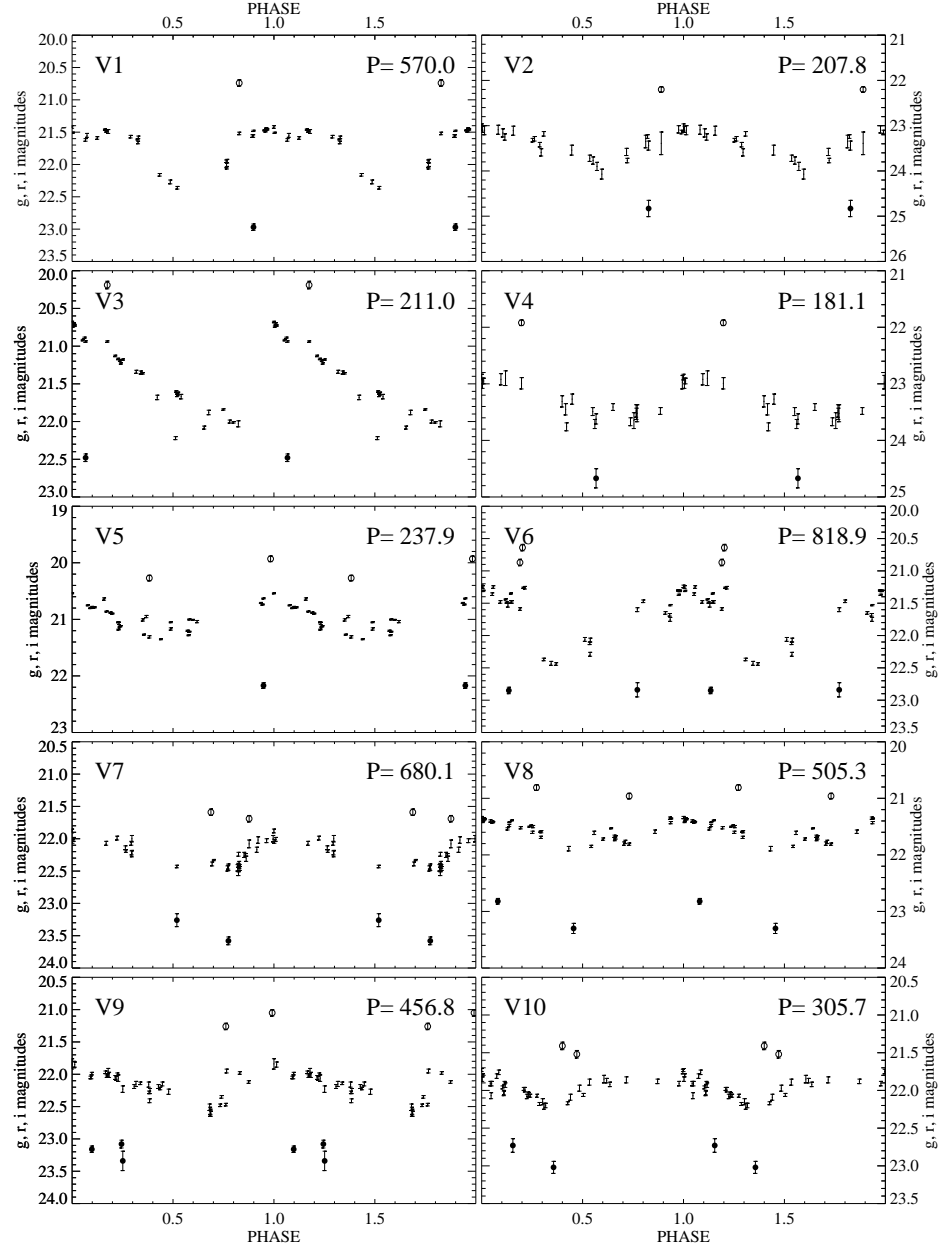


Fig. 3.— The light curves of the Long Period Variables in r (small dots with error bars), in g (large filled circles) and in i (large open circles). The identification numbers (V1-V37) and its periods are displayed in each graph. The periods are given in days.

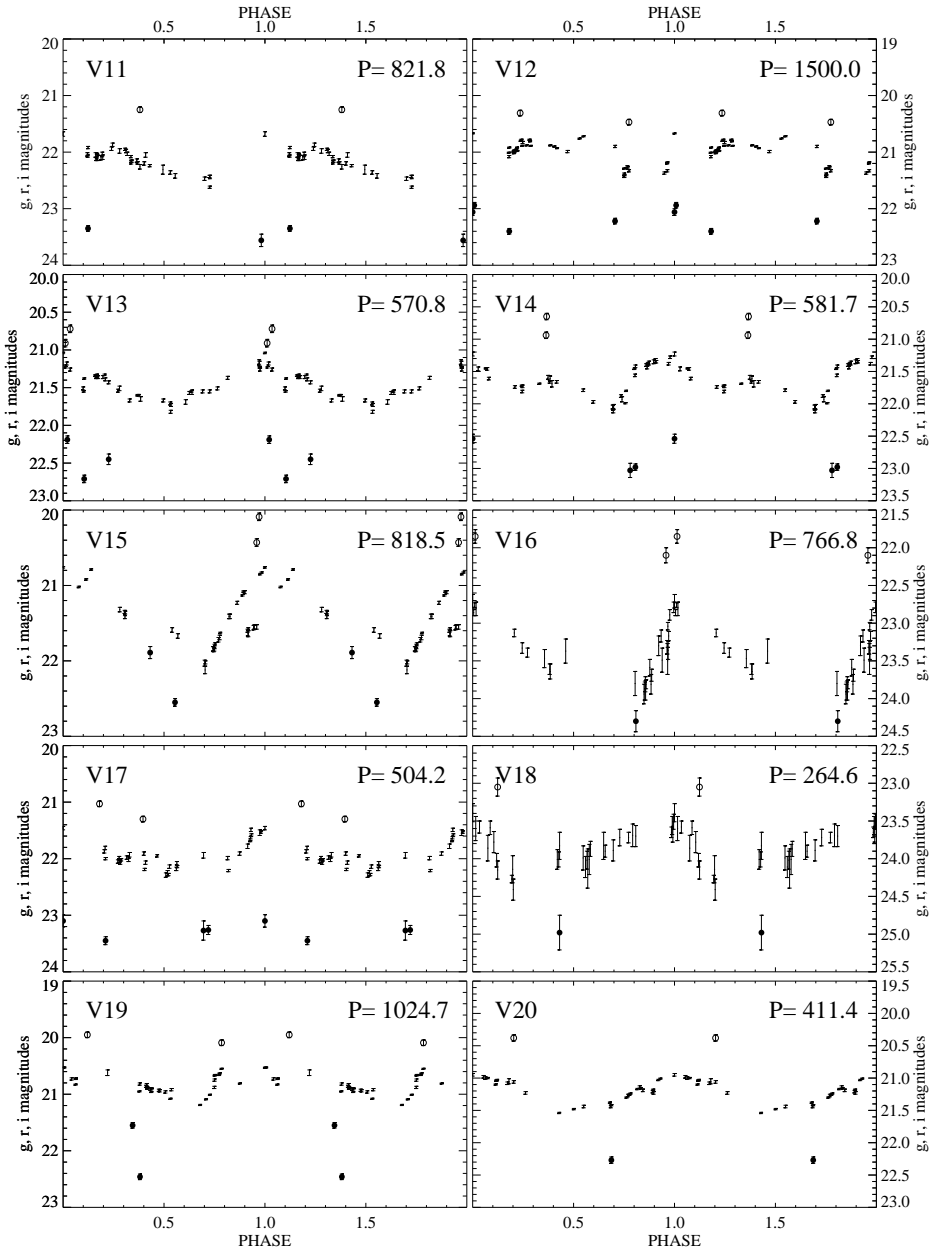


Fig. 3.— (contd.)

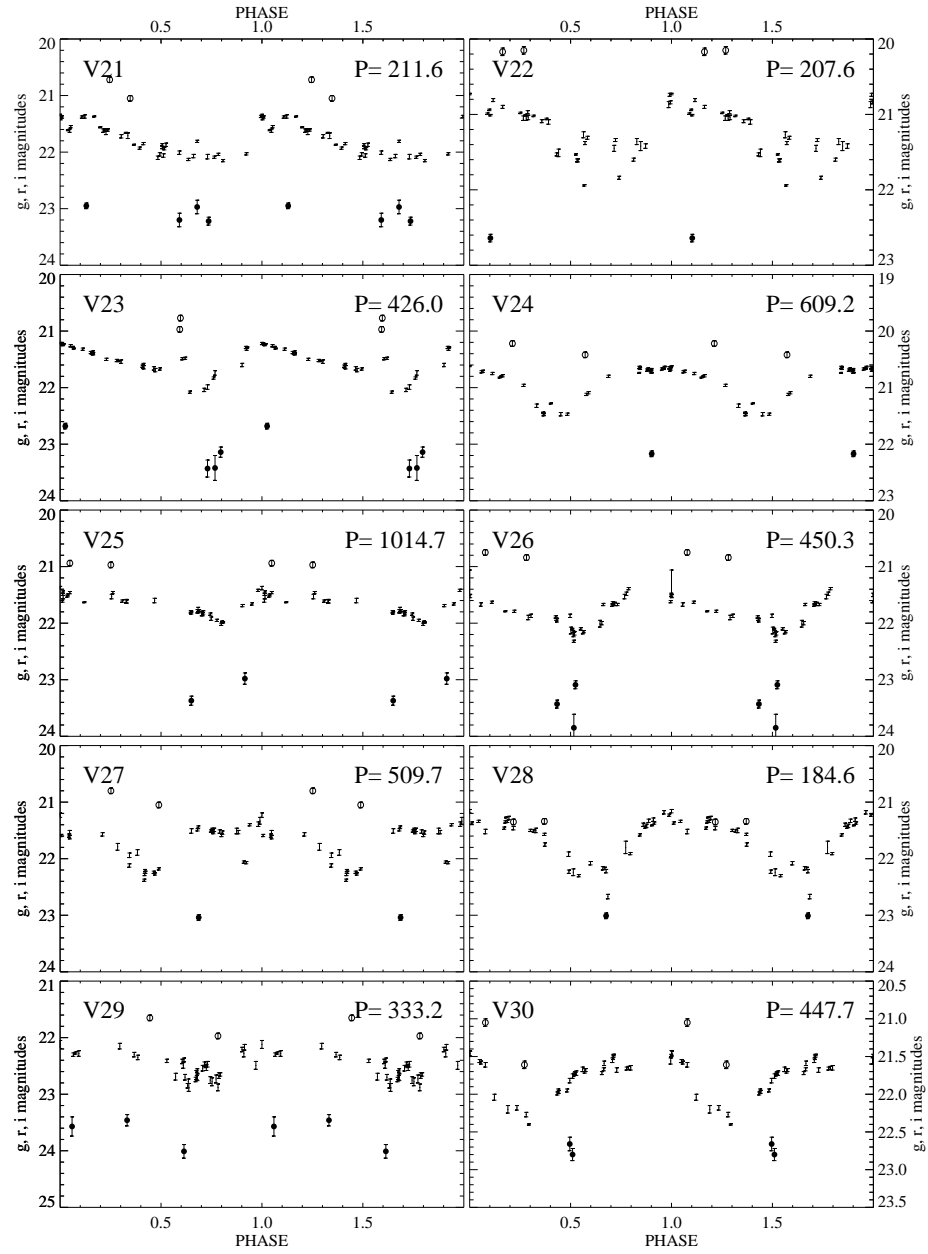


Fig. 3.— (contd.)

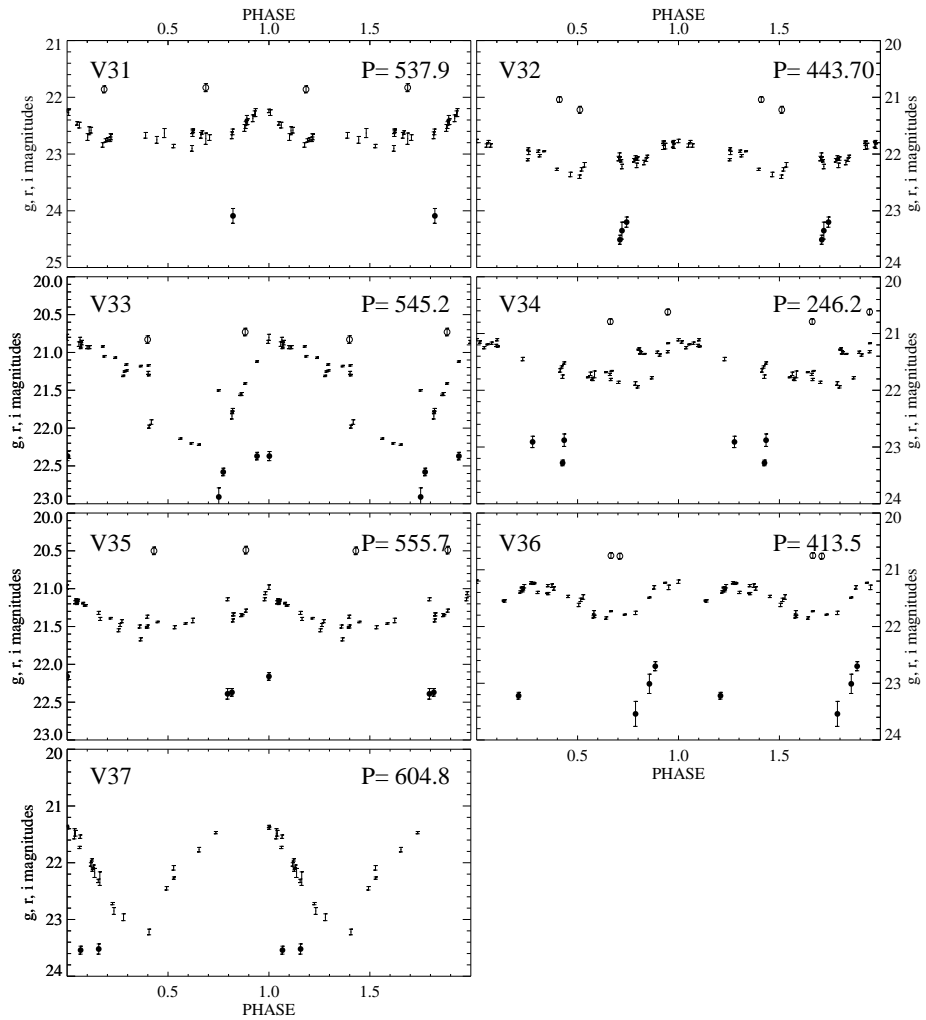


Fig. 3.— (contd.)

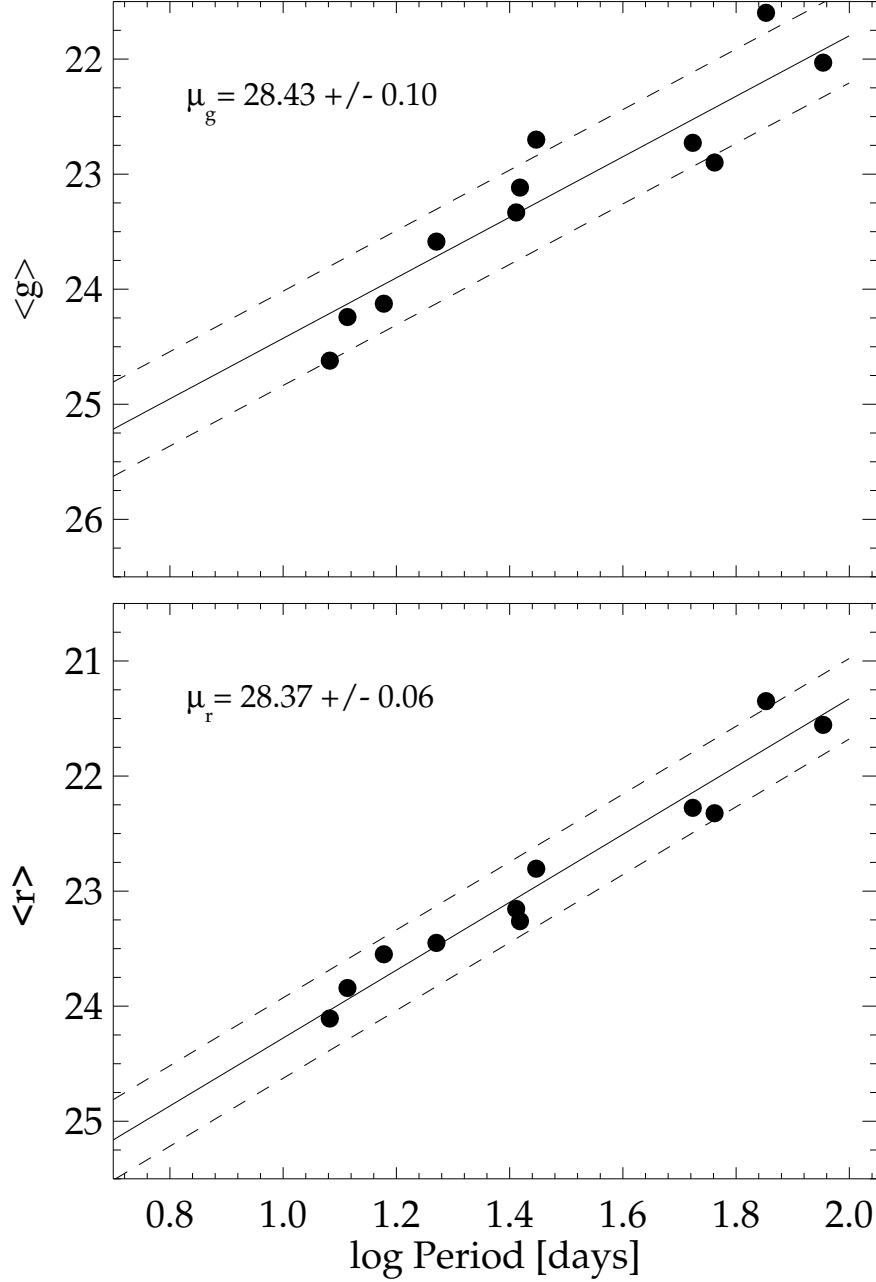


Fig. 4.— Period-luminosity relation of NGC4395 in g (top) and r (bottom) for all 11 Cepheids. The solid lines represent the best fit with the slope of -2.63 in g and -2.95 in r from eq. 15 and 16. The dashed lines account for an adopted intrinsic width of the instability strip of ± 0.41 mag in g and ± 0.35 mag in r .

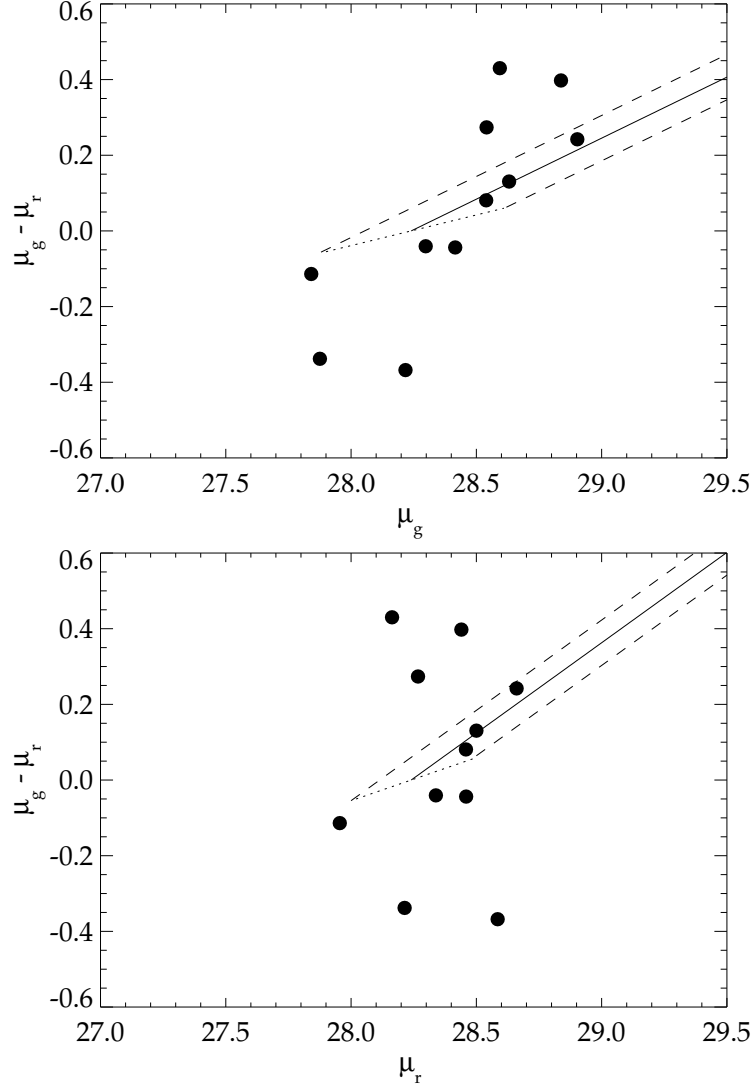


Fig. 5.— Individual apparent distance moduli μ_g (upper panel) and μ_r (lower panel) are plotted against the difference in the apparent distance moduli in g and r for each Cepheid, which allows to detect the presence of differential absorption. The bold lines indicates the reddening vectors, the dashed lines the width of the instability strip. With zero $E(g - r)$ reddening, the PL-relation is represented by a single point at $\mu_g = \mu_r = 28.22$. Because of the width of the instability strip this point is elongated and is shown as a dotted line in both figures. It is sloped due to the change of color across the instability strip, for details see Saha et al. (1996). The observed points in the upper panel are spread along a slope of 1 rather than on the reddening line, in the lower panel the points seems to spread in vertical direction. The distribution of the points illustrates that they do not lie on the reddening lines which indicates that there is no measurable differential absorption at the level of the

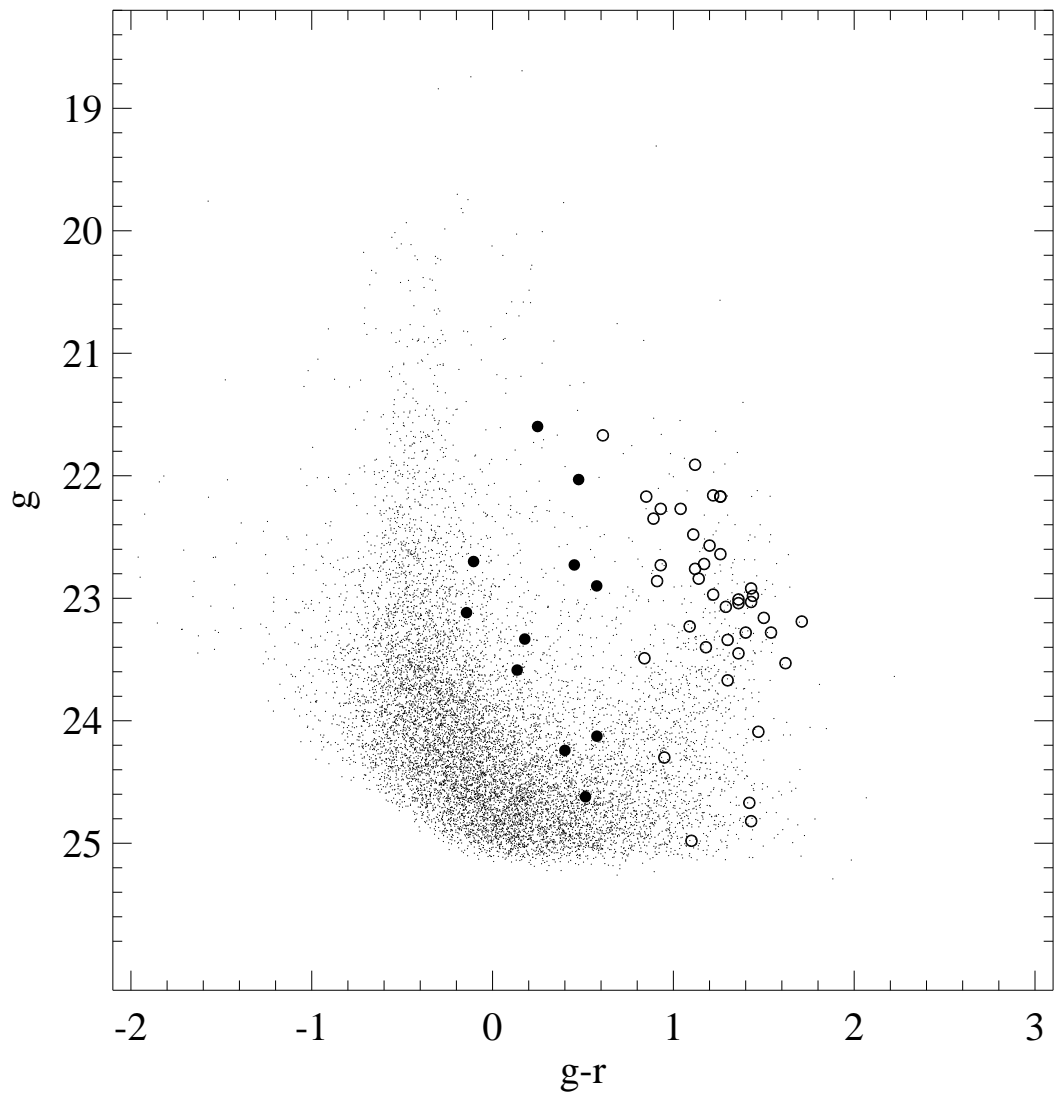


Fig. 6.— $g - r$ versus g color-magnitude diagram. Cepheids are plotted as filled circles, other variable candidates are plotted as open circles.

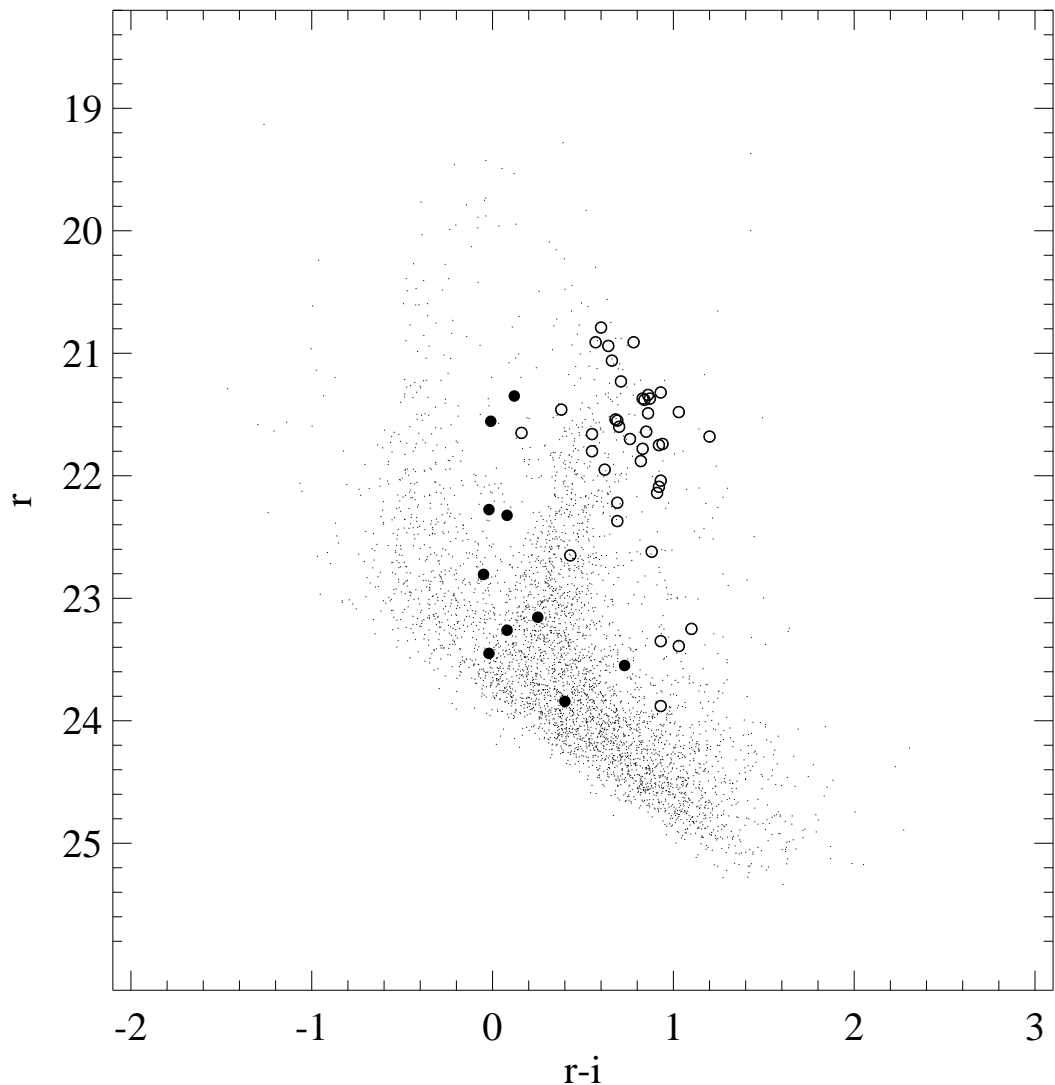


Fig. 7.— $r - i$ versus r color-magnitude diagram. Cepheids are plotted as filled circles, other variable candidates are plotted as open circles.

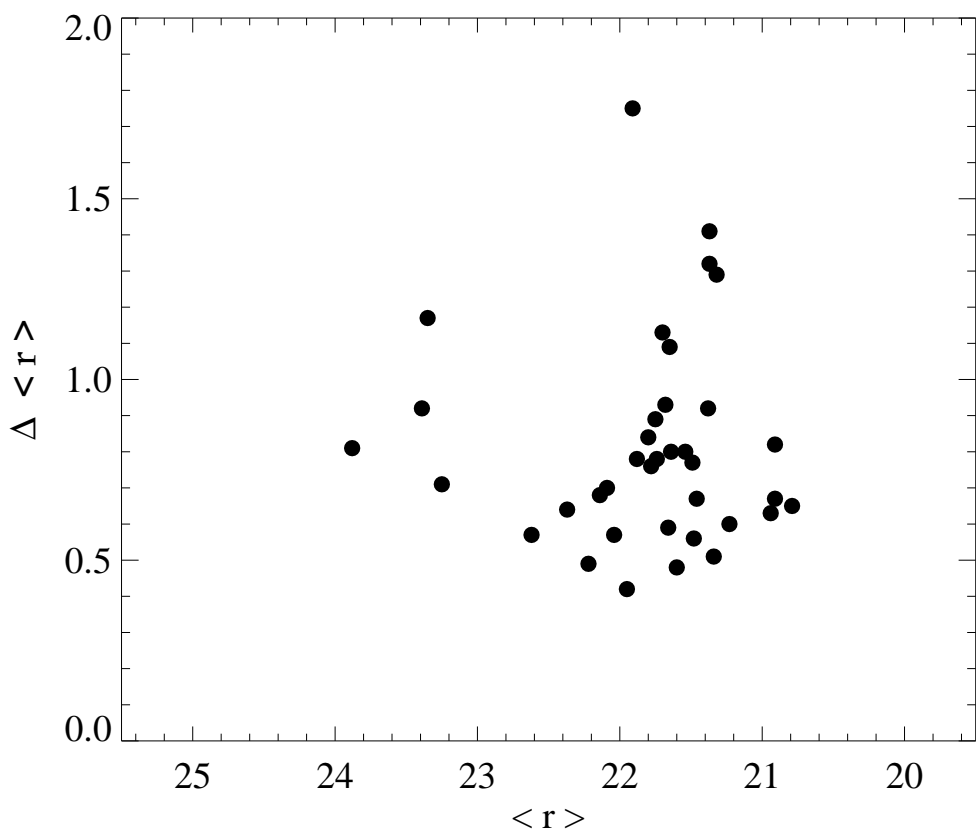


Fig. 8.— Mean r magnitudes for the long period variables are plotted against their r amplitude.

Table 1. Journal of Observations

Epoch (<i>HJD</i>) ^a	Exposure time [s]	Filter	Seeing [arc-sec]	Telescope	Instrument
48269.94	4 x 900	r	1.0	KP 2.1m	T1KA
48359.75	3 x 900	r	1.0	KP 2.1m	TI-2
48388.77	3 x 1200	r	1.0	KP 2.1m	TI-2
48622.95	3 x 900	r	1.3	KP 2.1m	T1KA
48622.95	2 x 900	g	1.2	KP 2.1m	T1KA
49064.83	3 x 1200	r	1.0	KP 2.1m	T1KA
49064.83	1 x 1200	g	1.0	KP 2.1m	T1KA
49076.86	3 x 900	g	1.2	KP 2.1m	T1KA
49417.87	4 x 600	i	1.5	KP 2.1m	T1KA
49421.84	3 x 900	r	1.1	KP 2.1m	T1KA
49427.87	3 x 900	r	1.0	KP 2.1m	T1KA
50189.89	900	r	0.76	WIYN	S2KB
50190.91	900	r	1.10	WIYN	S2KB
50191.71	900	r	0.90	WIYN	S2KB
50192.73	900	r	1.02	WIYN	S2KB
50213.83	900	r	1.08	WIYN	S2KB
50216.88	900	r	1.04	WIYN	S2KB
50226.64	900	i	0.94	WIYN	S2KB
50226.69	900	r	0.96	WIYN	S2KB

Table 1—Continued

Epoch (<i>HJD</i>) ^a	Exposure time [s]	Filter	Seeing [arc-sec]	Telescope	Instrument
50489.92	552	r	0.84	WIYN	S2KB
50509.77	1200	r	0.74	WIYN	S2KB
50510.95	1200	r	0.74	WIYN	S2KB
50511.79	1200	r	0.96	WIYN	S2KB
50834.05	900	r	0.72	WIYN	S2KB
50835.93	1200	r	1.18	WIYN	S2KB
50837.02	1200	r	0.72	WIYN	S2KB
50837.02	1500	g	0.68	WIYN	S2KB
50867.92	1200	r	0.92	WIYN	S2KB
50870.96	1200	r	0.86	WIYN	S2KB
50872.94	1200	r	0.88	WIYN	S2KB
50873.94	1200	r	0.92	WIYN	S2KB
50875.93	1200	r	0.68	WIYN	S2KB
50889.97	1200	r	0.86	WIYN	S2KB
50894.75	1200	r	0.78	WIYN	S2KB
50896.85	1200	r	0.74	WIYN	S2KB
50932.79	1200	r	0.86	WIYN	S2KB
50936.90	1200	r	1.08	WIYN	S2KB
50965.71	900	r	1.10	WIYN	S2KB

Table 1—Continued

Epoch (<i>HJD</i>) ^a	Exposure time [s]	Filter	Seeing [arc-sec]	Telescope	Instrument
50987.67	1200	r	0.86	WIYN	S2KB
50991.68	1200	r	0.72	WIYN	S2KB
50996.69	1200	r	1.06	WIYN	S2KB
51142.03	1200	r	0.78	WIYN	S2KB
51171.99	1200	r	0.92	WIYN	S2KB
51192.04	1200	r	0.68	WIYN	S2KB

^aHJD-2400000

Table 2. Local Standards

Identifier	<i>X</i>	<i>Y</i>	<i>g</i>	<i>r</i>	<i>i</i>	RA [J2000]	DEC [J2000]
A	1561	513	17.59	16.97	16.76	12:25:54.2	+33:31:40
B	1337	851	18.69	18.13	17.93	12:25:57.5	33:32:47
C	1116	850	18.49	18.20	18.09	12:26:01.2	33:32:48
D	694	1024	18.54	17.41	16.36	12:26:08.1	33:33:24
Z	1746	444	16.03	15.81	15.73	12:25:51.2	33:31:26
f1	472	1468	21.77	20.55	20.10	12:26:11.2	33:34:51
f2	148	972	20.94	20.12	19.78	12:26:17.3	33:33:16
f3	1210	1422	20.53	19.39	18.00	12:25:58.9	33:34:39

Table 3. Photometry of the Cepheids: Magnitudes and Error Estimates

HJD	C1	C2	C3	C4	C5	C6	C7	C8
<i>r</i>								
2448269.9406	23.81 0.16	...	21.30 0.03	23.98 0.18	23.15 0.10	23.23 0.08
2448359.7523	23.27 0.10
2448388.7788	23.18 0.12
2448622.9552	23.86 0.18	21.30 0.02	23.22 0.10	22.83 0.25	22.92 0.09
2449064.8339	21.39 0.02	22.86 0.07	22.93 0.08	22.62 0.08
2449421.8408	24.12 0.14	24.30 0.17	21.39 0.02	...	22.86 0.05	22.31 0.03 24.05 0.19
2449427.8788	23.07 0.06	21.41 0.01	22.85 0.05	23.06 0.05	22.58 0.04
2450189.8905	23.38 0.08	24.03 0.11	23.77 0.10	21.30 0.02	22.83 0.04	23.49 0.08	23.10 0.06	24.25 0.19
2450190.9141	22.95 0.09	21.30 0.02	22.95 0.09	23.31 0.13	23.05 0.09
2450191.7105	23.23 0.06	24.21 0.13	23.58 0.09	21.30 0.01	23.11 0.06	23.13 0.06	22.93 0.05	24.22 0.18
2450192.7317	23.11 0.10	24.05 0.18	21.30 0.02	23.12 0.09	22.97 0.08	22.97 0.09
2450213.8314	23.56 0.12	21.51 0.02	22.86 0.06	23.44 0.11	22.68 0.08
2450216.8806	21.46 0.02	22.74 0.07	23.00 0.08	22.76 0.06
2450226.6969	23.81 0.13	23.77 0.13	23.30 0.08	21.47 0.02	23.41 0.15	23.13 0.08	23.11 0.07	...
2450489.9295	23.11 0.09	24.09 0.22	21.39 0.02	23.19 0.09	23.35 0.12	22.61 0.06 24.01 0.22
2450509.7780	23.18 0.04	23.51 0.07	23.43 0.07	21.45 0.01	23.05 0.05	23.05 0.05	23.50 0.08	24.46 0.19
2450510.9513	23.30 0.06	23.67 0.08	23.17 0.06	21.52 0.02	23.21 0.05	23.03 0.05	23.00 0.05	23.65 0.10
2450511.7910	23.17 0.09	23.84 0.14	23.21 0.08	21.41 0.02	23.11 0.06	23.10 0.07	22.59 0.04	23.72 0.16
2450834.0550	23.78 0.16	23.45 0.11	23.75 0.14	21.31 0.02	23.58 0.12	23.57 0.12	22.97 0.07	...
2450835.9316	23.76 0.16	23.75 0.15	23.97 0.22	21.35 0.02	23.59 0.12	23.18 0.08	22.94 0.08	...
2450837.0266	23.77 0.08	23.72 0.07	23.83 0.08	21.31 0.01	23.41 0.05	22.99 0.04	23.12 0.04	24.53 0.18
2450867.9278	23.18 0.08	23.85 0.14	23.68 0.12	21.49 0.02	23.62 0.11	22.88 0.06	23.09 0.07	23.98 0.17
2450870.9631	23.44 0.06	23.80 0.09	23.47 0.07	21.45 0.01	22.93 0.05	22.91 0.04	23.24 0.06	...
2450872.9496	23.65 0.09	23.57 0.08	23.11 0.05	21.39 0.01	22.88 0.05	23.02 0.06	23.34 0.06	24.57 0.23
2450873.9432	23.56 0.10	23.40 0.09	23.30 0.11	21.40 0.02	22.90 0.05	23.07 0.07	23.24 0.09	23.89 0.15
2450875.9306	23.88 0.08	23.80 0.06	23.46 0.05	21.35 0.01	23.03 0.04	23.22 0.04	22.35 0.03	23.83 0.09
2450889.9782	24.18 0.23	23.40 0.12	21.26 0.02	23.52 0.13	22.90 0.07	23.05 0.09
2450894.7555	23.85 0.13	23.89 0.15	...	21.24 0.02	23.28 0.09	22.90 0.07	23.31 0.09	...
2450896.8575	23.84 0.08	23.71 0.06	23.84 0.07	21.23 0.01	22.93 0.04	22.89 0.04	23.11 0.05	24.34 0.17
2450932.7955	23.88 0.12	24.19 0.16	23.06 0.07	21.44 0.02	23.09 0.06	23.45 0.10	22.28 0.03	...
2450936.9023	23.24 0.11	23.58 0.17	21.40 0.03	23.48 0.14	23.55 0.17	22.50 0.07 23.75 0.20
2450965.7179	23.52 0.12	23.40 0.11	21.24 0.02	23.67 0.14	23.20 0.13	22.52 0.05
2450987.6717	23.78 0.11	23.77 0.09	23.92 0.12	21.38 0.01	23.26 0.05	23.56 0.09	22.57 0.04	24.33 0.17
2450991.6879	23.69 0.06	23.72 0.06	23.36 0.05	21.41 0.01	23.44 0.05	23.09 0.04	22.53 0.03	24.57 0.15
2450996.6918	23.30 0.14	23.34 0.14	21.49 0.03	23.75 0.20	22.93 0.09	22.71 0.07 23.67 0.20
2451142.0300	23.32 0.06	24.06 0.11	23.43 0.06	21.47 0.01	23.11 0.05	23.42 0.07	22.97 0.05	23.84 0.11
2451171.9956	23.59 0.10	23.57 0.08	23.38 0.06	21.26 0.01	23.30 0.06	23.16 0.06	23.11 0.06	24.40 0.18
2451192.0452	23.82 0.06	24.18 0.09	23.36 0.05	21.30 0.01	23.12 0.04	23.56 0.05	22.58 0.03	24.05 0.09
<i>g</i>								
2448622.9572	21.45 0.05	23.52 0.15	22.72 0.09	23.09 0.11
2449064.8359	21.60 0.05	22.78 0.11
2449076.8680	23.89 0.15	21.78 0.05	...	24.01 0.16	23.82 0.13
2450837.0286	24.19 0.12	24.16 0.12	24.59 0.18	21.67 0.05	24.01 0.10	23.16 0.05	23.66 0.07	24.21 0.13

Table 3—Continued

<i>i</i>												
HJD	C9	C10	C11	
2449417.8790	22.91	0.13	21.11	0.05	22.81	0.14	
2450226.6444	23.58	0.19	23.50	0.18	23.26	0.14	21.45	0.05	23.24	0.16	22.83	0.09
<i>r</i>												
2448269.9406	22.15	0.04	22.05	0.04	21.51	0.02	
2448359.7523	
2448388.7788	
2448622.9552	22.27	0.04	22.61	0.06	21.46	0.04	
2449064.8339	22.47	0.09	22.05	0.04	21.46	0.04	
2449421.8408	22.14	0.04	22.52	0.04	
2449427.8788	22.14	0.04	22.12	0.03	21.43	0.01	
2450189.8905	22.35	0.04	
2450190.9141	22.26	0.05	22.34	0.05	21.73	0.03	
2450191.7105	22.26	0.04	22.26	0.03	21.75	0.02	
2450192.7317	22.30	0.06	22.27	0.05	21.84	0.03	
2450213.8314	22.59	0.05	22.49	0.04	21.49	0.02	
2450216.8806	22.59	0.06	22.38	0.05	21.42	0.02	
2450226.6969	22.15	0.04	21.99	0.03	21.35	0.02	
2450489.9295	22.43	0.05	22.08	0.04	21.48	0.02	
2450509.7780	22.49	0.04	22.27	0.02	21.50	0.02	
2450510.9513	22.38	0.04	22.26	0.03	21.39	0.01	
HJD	C9	C10	C11	
<i>r</i>												
2450511.7910	22.30	0.04	22.38	0.04	21.51	0.02	
2450834.0550	22.38	0.04	22.42	0.04	21.65	0.02	
2450835.9316	22.38	0.04	22.45	0.05	21.56	0.05	
2450837.0266	22.47	0.04	22.55	0.03	
2450867.9278	22.09	0.04	22.10	0.03	21.45	0.02	
2450870.9631	22.12	0.04	22.07	0.02	21.39	0.01	
2450872.9496	22.09	0.02	22.15	0.02	21.48	0.01	
2450873.9432	22.10	0.04	22.16	0.03	21.46	0.01	
2450875.9306	22.17	0.02	22.18	0.02	21.45	0.01	
2450889.9782	22.38	0.05	22.49	0.06	21.57	0.03	
2450894.7555	22.40	0.04	22.59	0.05	21.63	0.02	
2450896.8575	22.44	0.04	22.61	0.03	21.64	0.01	
2450932.7955	22.10	0.04	22.27	0.04	21.38	0.02	
2450936.9023	22.24	0.05	22.38	0.06	21.42	0.03	
2450965.7179	22.55	0.05	22.03	0.03	21.47	0.02	
2450987.6717	22.18	0.04	22.38	0.03	21.80	0.02	
2450991.6879	22.18	0.02	22.38	0.02	21.71	0.01	
2450996.6918	22.14	0.04	22.43	0.06	21.72	0.03	
2451142.0300	22.61	0.04	22.27	0.03	21.53	0.01	
2451171.9956	22.22	0.04	22.23	0.03	21.80	0.02	
2451192.0452	22.59	0.04	22.17	0.02	21.66	0.01	

Table 3—Continued

<i>g</i>				
2448622.9572	22.61 0.09	23.15 0.11	21.91 0.05	
2449064.8359	23.18 0.19	22.41 0.08
2449076.8680	22.50 0.05	22.72 0.05	21.93 0.05	
2450837.0286	23.15 0.05	23.15 0.05	22.18 0.05	
<i>i</i>				
2449417.8790	22.11 0.08	22.59 0.09	21.40 0.05	
2450226.6444	22.15 0.05	22.05 0.05	21.40 0.05	

Table 4. Photometry of the Variable Stars: Magnitudes and Error Estimates

HJD	V1	V2	V3	V4	V5	V6	V7	V8
<i>r</i>								
2448269.9406	20.64 0.02	21.47 0.02	21.88 0.03	21.59 0.03
2448359.7523	21.65 0.02
2448388.7788
2448622.9552	22.43 0.06	21.61 0.03
2449064.8339	21.60 0.03	22.07 0.04	21.89 0.04
2449421.8408	20.55 0.01	21.26 0.01	22.39 0.03	21.42 0.01
2449427.8788	21.26 0.02	22.33 0.03	21.39 0.01
2450189.8905	21.95 0.02	...	20.68 0.01	22.97 0.05	21.05 0.01	21.35 0.01	22.41 0.04	21.67 0.02
2450190.9141	22.01 0.04	23.58 0.14	20.74 0.01	22.88 0.09	21.07 0.02	21.48 0.02	22.24 0.05	21.72 0.03
2450191.7105	22.05 0.02	23.77 0.10	20.70 0.01	22.99 0.05	21.13 0.01	21.48 0.02	22.46 0.03	21.70 0.02
2450192.7317	21.95 0.04	...	20.73 0.01	22.95 0.10	21.12 0.01	21.48 0.02	22.38 0.05	21.69 0.03
2450213.8314	21.80 0.03
2450216.8806	21.77 0.03
2450226.6969	21.52 0.02	23.39 0.09	20.94 0.01	22.99 0.07	21.31 0.02	21.59 0.02	22.08 0.03	21.81 0.02
2450489.9295	21.57 0.02	23.11 0.08	21.68 0.03	23.41 0.10	21.17 0.02	22.06 0.03	22.14 0.03	21.60 0.02
2450509.7780	21.61 0.01	23.32 0.07	21.60 0.01	...	21.20 0.01	22.12 0.02	22.07 0.02	21.59 0.01
2450510.9513	21.66 0.02	...	21.63 0.01	23.53 0.09	21.28 0.01	22.30 0.03	22.22 0.03	21.69 0.02
2450511.7910	21.58 0.02	23.30 0.08	21.63 0.02	...	21.22 0.01	22.07 0.03	22.00 0.03	21.59 0.02
2450834.0550	21.56 0.02	23.35 0.10	20.92 0.01	23.49 0.11	20.71 0.01	21.68 0.02	22.46 0.05	21.35 0.02
2450835.9316	21.56 0.02	23.24 0.10	20.89 0.01	23.71 0.15	20.74 0.01	21.75 0.03	22.44 0.05	21.43 0.02
2450837.0266	21.48 0.01	23.44 0.05	20.94 0.01	23.62 0.06	20.63 0.01	21.53 0.01	22.44 0.03	21.36 0.01
2450867.9278	21.47 0.01	23.08 0.07	21.13 0.01	23.67 0.13	20.75 0.01	21.30 0.01	22.45 0.03	21.34 0.02
2450870.9631	21.49 0.01	23.14 0.05	21.17 0.01	23.65 0.10	20.80 0.01	21.38 0.01	22.55 0.04	21.42 0.01
2450872.9496	21.44 0.01	23.05 0.04	21.19 0.01	23.48 0.07	20.78 0.01	21.31 0.01	22.42 0.03	21.38 0.01
2450873.9432	21.46 0.01	23.08 0.05	21.23 0.01	23.52 0.10	20.80 0.01	21.31 0.01	22.43 0.03	21.35 0.01
2450875.9306	21.46 0.01	23.10 0.04	21.18 0.01	...	20.80 0.01	21.31 0.01	22.46 0.02	21.38 0.01
2450889.9782	23.09 0.10	21.34 0.02	...	20.86 0.01	21.24 0.02	22.25 0.05
2450894.7555	21.42 0.02	23.16 0.08	21.35 0.02	23.48 0.12	20.88 0.01	21.25 0.02	22.25 0.03	21.42 0.02
2450896.8575	21.51 0.01	23.25 0.04	21.36 0.01	...	20.90 0.01	21.31 0.01	22.31 0.03	21.42 0.01
2450932.7955	21.62 0.02	23.42 0.08	21.65 0.02	22.92 0.06	21.01 0.02	21.36 0.02	22.17 0.03	21.55 0.02
2450936.9023	21.55 0.04	23.18 0.11	21.67 0.03	22.90 0.10	20.95 0.02	21.25 0.02	22.02 0.05	21.48 0.02
2450965.7179	21.59 0.02	23.55 0.11	21.88 0.03	...	21.05 0.01	21.48 0.02	22.03 0.03	21.52 0.02
2450987.6717	21.46 0.01	23.77 0.09	22.00 0.02	23.31 0.08	21.00 0.01	21.44 0.01	22.00 0.02	21.50 0.01
2450991.6879	21.49 0.01	23.90 0.08	22.01 0.01	23.76 0.07	21.01 0.01	21.49 0.01	22.05 0.01	21.48 0.01
2450996.6918	21.49 0.04	24.07 0.25	22.03 0.04	23.27 0.14	21.05 0.02	21.53 0.03	22.01 0.05	21.50 0.02
2451142.0300	22.16 0.02	23.59 0.07	22.22 0.02	...	21.18 0.01	22.38 0.02	21.99 0.02	21.85 0.02
2451171.9956	22.27 0.04	...	22.08 0.02	23.45 0.09	21.27 0.01	22.43 0.03	22.19 0.04	21.72 0.02
2451192.0452	22.36 0.02	23.72 0.05	21.84 0.01	...	21.35 0.01	22.44 0.02	22.23 0.02	21.53 0.01
<i>g</i>								
2448622.9572	23.26 0.10	...
2449064.8359	22.84 0.11
2449076.8680	23.30 0.09
2450837.0286	22.97 0.05	24.83 0.18	22.48 0.05	24.67 0.17	22.17 0.05	22.85 0.05	23.58 0.06	22.82 0.05

Table 4—Continued

<i>i</i>																
2449417.8790	19.93	0.05	20.64	0.05	21.59	0.05	20.81	0.05		
2450226.6444	20.74	0.05	22.20	0.06	20.19	0.05	21.92	0.05	20.27	0.05	20.88	0.05	21.69	0.05	20.96	0.05
HJD	V9	V10	V11	V12	V13	V14	V15	V16								
<i>r</i>																
2448269.9406	22.27	0.05	21.86	0.03	21.68	0.02	20.99	0.02	21.69	0.02	21.69	0.03	21.67	0.03	23.38	0.16
2448359.7523	20.76	0.01	21.51	0.03	21.80	0.03
2448388.7788	20.72	0.01	21.38	0.03	21.97	0.04
2448622.9552	22.23	0.05	21.88	0.03	22.24	0.04	20.90	0.02	21.43	0.02	21.23	0.02	20.76	0.01	23.30	0.13
2449064.8339	22.06	0.04	22.20	0.04	20.67	0.01	21.05	0.02	21.80	0.04	21.59	0.03
2449421.8408	21.84	0.02	21.97	0.03	22.20	0.03	20.80	0.01	21.57	0.02	21.59	0.02	20.85	0.01	23.32	0.09
2449427.8788	21.85	0.02	22.06	0.03	22.05	0.03	20.78	0.01	21.55	0.02	21.61	0.02	20.83	0.01	23.17	0.06
2450189.8905	22.51	0.04	21.75	0.02	22.08	0.03	21.30	0.01	21.16	0.01	22.05	0.02	21.60	0.02	23.34	0.07
2450190.9141	22.58	0.09	21.73	0.03	22.18	0.04	21.39	0.02	21.18	0.02	22.06	0.05	21.63	0.04	23.50	0.18
2450191.7105	22.58	0.04	21.85	0.02	22.16	0.03	21.43	0.02	21.23	0.01	22.11	0.03	21.58	0.02	23.05	0.05
2450192.7317	22.61	0.05	21.80	0.03	22.16	0.05	21.42	0.02	21.26	0.02	22.05	0.04	21.64	0.04	23.36	0.12
2450213.8314	22.48	0.08	21.81	0.03	22.15	0.04	21.26	0.02	21.23	0.02	21.88	0.03	21.56	0.03	22.80	0.07
2450216.8806	22.35	0.04	21.76	0.03	22.19	0.04	21.28	0.02	21.18	0.02	21.93	0.04	21.55	0.03	22.71	0.09
2450226.6969	22.47	0.04	21.93	0.03	22.26	0.04	21.33	0.02	21.26	0.02	21.99	0.03	21.55	0.03
2450489.9295	22.14	0.04	21.91	0.04	22.47	0.08	21.38	0.02	21.67	0.03	21.74	0.03	21.32	0.03	23.47	0.12
2450509.7780	22.28	0.02	21.91	0.02	22.43	0.03	21.20	0.01	21.71	0.02	21.72	0.02	21.35	0.02	23.61	0.07
2450510.9513	22.41	0.04	22.07	0.03	22.62	0.04	21.33	0.02	21.82	0.02	21.81	0.02	21.42	0.02
HJD	V9	V10	V11	V12	V13	V14	V15	V16								
<i>r</i>																
2450511.7910	22.26	0.04	21.91	0.03	22.44	0.04	21.18	0.01	21.73	0.03	21.73	0.02	21.36	0.02	23.64	0.10
2450834.0550	22.05	0.04	21.96	0.03	22.05	0.03	21.01	0.01	21.51	0.02	21.46	0.02	22.03	0.04	23.80	0.16
2450835.9316	22.05	0.04	22.05	0.04	22.07	0.04	21.08	0.02	21.55	0.02	21.56	0.03	22.12	0.05
2450837.0266	21.99	0.02	21.90	0.02	21.92	0.02	20.92	0.01	21.38	0.01	21.42	0.01	22.02	0.02
2450867.9278	21.97	0.04	21.99	0.03	22.05	0.03	20.99	0.01	21.34	0.01	21.40	0.02	21.84	0.03	23.94	0.13
2450870.9631	22.03	0.02	22.08	0.03	22.12	0.02	21.02	0.01	21.38	0.01	21.44	0.02	21.85	0.03	23.90	0.12
2450872.9496	22.01	0.02	22.05	0.03	22.08	0.02	20.97	0.01	21.34	0.01	21.38	0.01	21.85	0.02	23.81	0.10
2450873.9432	21.95	0.02	22.06	0.03	22.05	0.03	21.01	0.01	21.36	0.02	21.39	0.02	21.81	0.03	23.89	0.13
2450875.9306	22.01	0.02	22.07	0.02	22.10	0.02	20.99	0.01	21.36	0.01	21.38	0.01	21.78	0.02	23.81	0.06
2450889.9782	22.05	0.04	22.18	0.04	22.10	0.04	20.95	0.01	21.36	0.02	21.35	0.02	21.72	0.03	23.59	0.11
2450894.7555	22.00	0.04	22.15	0.04	22.05	0.03	20.92	0.01	21.33	0.02	21.33	0.02	21.69	0.03	23.81	0.13
2450896.8575	22.06	0.02	22.21	0.02	22.09	0.02	20.98	0.01	21.39	0.01	21.35	0.01	21.63	0.01	23.69	0.08
2450932.7955	22.19	0.04	22.17	0.04	21.94	0.02	20.89	0.01	21.55	0.02	21.38	0.02	21.41	0.03	23.17	0.08
2450936.9023	22.15	0.04	22.09	0.05	21.88	0.03	20.83	0.02	21.51	0.03	21.28	0.02	21.41	0.03	23.49	0.16
2450965.7179	22.16	0.04	21.89	0.03	21.98	0.03	20.88	0.01	21.67	0.02	21.46	0.02	21.23	0.02	22.89	0.07
2450987.6717	22.19	0.02	21.85	0.02	21.95	0.02	20.78	0.01	21.60	0.01	21.45	0.01	21.13	0.01	22.86	0.04
2450991.6879	22.22	0.02	21.88	0.02	21.98	0.02	20.81	0.01	21.60	0.01	21.46	0.01	21.08	0.01	22.76	0.03
2450996.6918	22.15	0.04	21.92	0.04	22.03	0.04	20.89	0.01	21.65	0.03	21.61	0.03	21.09	0.02	22.81	0.09
2451142.0300	21.95	0.02	22.03	0.03	22.31	0.02	20.88	0.01	21.56	0.01	21.69	0.01	21.02	0.01	23.13	0.05
2451171.9956	21.98	0.02	21.98	0.02	22.36	0.03	20.90	0.01	21.55	0.02	21.66	0.02	20.92	0.01	23.33	0.07
2451192.0452	22.12	0.02	22.07	0.02	22.42	0.03	20.93	0.01	21.55	0.01	21.66	0.01	20.80	0.01	23.39	0.06

Table 4—Continued

<i>g</i>									
HJD	V17	V18	V19	V20	V21	V22	V23	V24	
<i>i</i>									
2448622.9572	23.34 0.16	22.73 0.09	22.22 0.05	22.45 0.07	22.55 0.07	21.89 0.08
2449064.8359	22.06 0.06
2449076.8680	23.08 0.06	23.02 0.08	23.56 0.11	21.94 0.05	22.19 0.05	23.03 0.11	22.55 0.05
2450837.0286	23.16 0.05	...	23.35 0.05	22.40 0.05	22.71 0.05	22.98 0.05	...	24.30 0.14	
<i>r</i>									
2448269.9406	...	23.72 0.14	20.81 0.01	...	22.03 0.03	21.84 0.05	21.60 0.03	20.80 0.02	
2448359.7523
2448388.7788	22.10 0.05
2448622.9552	22.21 0.05	...	20.62 0.05	...	22.01 0.04	21.51 0.04	21.99 0.04	20.96 0.02	
2449064.8339	21.94 0.04	21.81 0.03	21.94 0.06	21.74 0.04	20.69 0.02	
2449421.8408	22.19 0.04	...	20.53 0.01	...	21.88 0.03	20.97 0.03	21.49 0.02	21.12 0.02	
2449427.8788	...	23.78 0.10	20.53 0.01	21.23 0.01	21.93 0.02	21.02 0.03	21.48 0.02	21.09 0.02	
2450189.8905	21.69 0.02	23.65 0.10	20.88 0.02	21.10 0.02	21.38 0.02	20.88 0.02	21.62 0.02	20.74 0.01	
2450190.9141	21.63 0.04	23.56 0.17	20.75 0.02	21.05 0.02	21.35 0.02	20.74 0.02	21.63 0.03	20.64 0.02	
2450191.7105	21.49 0.02	23.61 0.09	20.67 0.01	21.05 0.01	21.41 0.01	20.84 0.01	21.59 0.02	20.65 0.02	
2450192.7317	21.58 0.05	23.51 0.12	20.66 0.01	21.03 0.01	21.38 0.02	20.73 0.02	21.64 0.03	20.66 0.02	
2450213.8314	21.55 0.02	23.86 0.14	20.66 0.01	21.08 0.01	21.38 0.03	...	21.66 0.03	20.69 0.02	
2450216.8806	21.53 0.04	23.59 0.13	20.63 0.01	21.05 0.02	21.38 0.02	20.81 0.02	21.69 0.03	20.67 0.02	
2450226.6969	21.46 0.02	24.15 0.16	20.55 0.01	21.06 0.02	21.38 0.02	20.90 0.02	21.67 0.02	20.68 0.01	
2450489.9295	22.28 0.04	24.02 0.18	20.73 0.02	21.19 0.02	21.85 0.03	21.53 0.03	21.32 0.02	21.32 0.03	
2450509.7780	22.18 0.04	24.27 0.14	20.83 0.01	21.21 0.01	21.92 0.02	21.53 0.02	21.39 0.02	21.44 0.01	
2450510.9513	22.08 0.04	24.14 0.12	20.72 0.01	21.18 0.01	22.06 0.02	21.61 0.02	21.41 0.01	21.48 0.02	
2450511.7910	22.14 0.04	24.41 0.26	20.73 0.01	21.23 0.01	21.94 0.03	21.61 0.04	21.40 0.02	21.47 0.02	
2450834.0550	21.88 0.04	24.01 0.20	20.95 0.01	21.38 0.02	21.61 0.03	20.99 0.02	21.30 0.02	20.71 0.01	
2450835.9316	21.81 0.04	24.01 0.18	20.82 0.02	21.44 0.04	21.62 0.02	20.94 0.02	21.32 0.02	20.68 0.02	
2450837.0266	22.00 0.02	23.83 0.08	...	21.42 0.02	21.55 0.01	21.01 0.01	21.30 0.01	20.74 0.01	
2450867.9278	22.05 0.04	23.99 0.15	20.86 0.02	21.30 0.02	21.56 0.02	20.98 0.01	21.22 0.02	20.67 0.02	
2450870.9631	21.98 0.04	24.11 0.14	20.83 0.02	21.27 0.02	21.62 0.02	21.05 0.01	21.22 0.01	20.66 0.01	
2450872.9496	22.05 0.02	24.02 0.12	20.89 0.02	21.26 0.01	21.61 0.01	21.01 0.01	21.24 0.01	20.67 0.01	
2450873.9432	22.07 0.04	24.13 0.16	20.89 0.02	21.26 0.02	21.64 0.02	21.05 0.01	21.25 0.01	20.67 0.01	
2450875.9306	22.02 0.02	24.01 0.08	20.89 0.01	21.24 0.01	21.61 0.01	21.05 0.01	21.23 0.01	20.63 0.01	
2450889.9782	21.98 0.04	...	20.91 0.02	21.17 0.02	21.72 0.03	21.09 0.03	21.26 0.02	20.65 0.02	
2450894.7555	22.02 0.04	23.83 0.14	20.96 0.01	21.14 0.01	21.66 0.02	21.06 0.02	21.28 0.01	20.67 0.02	
2450896.8575	21.93 0.02	23.90 0.07	20.90 0.01	21.16 0.01	21.71 0.01	21.10 0.01	21.31 0.01	20.62 0.01	
2450932.7955	21.91 0.04	23.69 0.12	20.93 0.02	21.03 0.01	21.88 0.02	21.27 0.03	21.38 0.02	20.72 0.02	
2450936.9023	22.07 0.04	23.70 0.17	20.94 0.02	21.01 0.02	21.88 0.03	21.31 0.04	21.38 0.02	20.71 0.02	
2451142.0300	21.99 0.02	23.88 0.10	21.19 0.01	21.55 0.01	22.05 0.02	21.38 0.02	22.08 0.02	21.28 0.01	
2451171.9956	21.91 0.02	23.89 0.11	21.09 0.01	21.48 0.01	22.13 0.02	21.45 0.02	22.05 0.03	21.47 0.03	
2451192.0452	21.78 0.01	23.72 0.07	21.01 0.01	21.44 0.01	22.08 0.02	21.60 0.01	21.83 0.02	21.47 0.02	

Table 4—Continued

<hr/>									
<i>r</i>									
2450965.7179	21.95 0.04	20.96 0.02	20.95 0.01	22.07 0.03	21.34 0.02	21.50 0.02	20.75 0.02
2450987.6717	22.30 0.04	23.39 0.09	20.98 0.01	22.09 0.02	21.36 0.02	21.52 0.02	20.82 0.01
2450991.6879	22.26 0.02	23.60 0.05	21.08 0.01	21.00 0.01	22.05 0.02	21.42 0.01	21.53 0.01	20.80 0.01	
2450996.6918	22.14 0.05	23.58 0.18	20.92 0.02	21.00 0.02	22.15 0.05	21.42 0.04	21.55 0.03	20.80 0.02	
<hr/>									
<i>g</i>									
2448622.9572	23.10 0.12	21.55 0.05	23.20 0.12
2449064.8359	23.27 0.17	22.97 0.12
2449076.8680	23.26 0.09	23.22 0.07
2450837.0286	23.45 0.08	24.98 0.23	22.46 0.05	22.27 0.05	22.95 0.05	22.64 0.05	22.68 0.05	22.17 0.05	
<hr/>									
<i>i</i>									
2449417.8790	21.30 0.05	19.95 0.05	21.05 0.05	20.15 0.05	20.77 0.05
2450226.6444	21.03 0.05	23.05 0.12	20.09 0.05	20.38 0.05	20.72 0.05	20.17 0.05	20.97 0.05	20.22 0.05	
<hr/>									
HJD	V25	V26	V27	V28	V29	V30	V31	V32	
<hr/>									
<i>r</i>									
2448269.9406	21.63 0.04	21.67 0.03	21.51 0.03	21.80 0.04	22.28 0.06	21.55 0.03	22.46 0.06	21.80 0.04	
2448359.7523	
2448388.7788	
2448622.9552	21.60 0.04	22.32 0.06	22.12 0.05	22.67 0.11	22.49 0.07	21.82 0.03	22.71 0.07	22.22 0.05	
2449064.8339	21.69 0.04	21.88 0.04	21.57 0.03	21.52 0.03	22.15 0.05	21.95 0.04	22.86 0.10	22.12 0.05	
2449421.8408	21.53 0.02	21.90 0.02	22.06 0.04	21.38 0.03	22.30 0.04	22.27 0.04	22.76 0.05	22.27 0.04	
2449427.8788	21.46 0.02	21.88 0.02	22.07 0.03	21.34 0.02	22.35 0.04	22.40 0.05	22.74 0.06	22.19 0.03	
2450189.8905	21.60 0.02	21.62 0.02	22.38 0.04	21.46 0.02	22.74 0.04	21.56 0.02	22.90 0.05	...	
2450190.9141	21.49 0.04	21.50 0.03	22.28 0.06	21.35 0.03	22.66 0.08	21.49 0.03	22.60 0.07	22.10 0.05	
2450191.7105	21.45 0.01	21.28 0.22	22.21 0.04	21.27 0.02	22.71 0.04	21.46 0.01	22.64 0.03	21.91 0.02	
2450192.7317	21.55 0.04	21.52 0.03	22.24 0.06	21.34 0.03	22.70 0.06	21.46 0.03	22.59 0.05	21.98 0.04	
2450213.8314	21.52 0.02	22.24 0.04	21.50 0.03	22.75 0.06	21.56 0.03	22.67 0.05	21.95 0.04
2450216.8806	21.50 0.02	21.67 0.03	22.27 0.05	21.51 0.03	22.78 0.07	21.58 0.03	22.62 0.06	22.03 0.04	
2450226.6969	21.46 0.02	22.18 0.04	21.57 0.03	22.88 0.06	21.61 0.02	22.73 0.05	21.95 0.03
2450489.9295	21.61 0.04	21.67 0.03	21.59 0.03	21.91 0.04	22.69 0.06	21.59 0.03	22.84 0.06	21.81 0.03	
2450509.7780	21.61 0.02	21.68 0.02	21.59 0.02	21.41 0.02	22.85 0.04	21.51 0.02	22.76 0.04	21.83 0.02	
2450510.9513	21.61 0.02	21.64 0.02	21.55 0.03	21.31 0.02	22.77 0.04	21.49 0.02	22.67 0.04	21.78 0.02	
2450511.7910	21.62 0.02	21.66 0.02	21.62 0.03	21.38 0.02	22.88 0.07	21.48 0.02	22.70 0.05	21.86 0.03	
2450834.0550	21.80 0.04	21.89 0.03	21.49 0.03	22.17 0.04	22.42 0.04	21.99 0.03	22.67 0.05	22.08 0.04	
2450835.9316	21.80 0.04	21.93 0.06	21.44 0.02	22.17 0.04	22.49 0.05	21.95 0.04	22.61 0.06	22.02 0.03	
2450837.0266	21.82 0.02	21.95 0.02	...	22.22 0.03	22.39 0.03	21.97 0.02	...	22.08 0.02	
2450867.9278	21.80 0.04	22.13 0.03	21.51 0.02	21.58 0.02	22.55 0.05	21.76 0.02	22.55 0.08	22.11 0.03	
2450870.9631	21.76 0.02	22.10 0.02	21.48 0.02	21.40 0.02	22.47 0.04	21.74 0.02	22.49 0.03	22.06 0.03	
2450872.9496	21.78 0.02	22.15 0.02	21.51 0.02	21.44 0.02	22.50 0.03	21.72 0.02	22.45 0.03	22.09 0.02	
2450873.9432	21.80 0.02	22.20 0.03	21.55 0.02	21.42 0.02	22.53 0.05	21.73 0.02	22.36 0.03	22.20 0.03	
2450875.9306	21.78 0.02	22.18 0.03	21.49 0.02	21.33 0.01	22.47 0.05	21.72 0.02	22.43 0.03	22.08 0.02	
2450889.9782	21.83 0.04	22.10 0.04	21.52 0.02	21.18 0.02	22.73 0.07	21.67 0.03	22.38 0.05	22.15 0.04	
2450894.7555	21.84 0.04	22.16 0.03	21.58 0.02	21.23 0.02	22.67 0.05	21.69 0.03	22.30 0.04	22.10 0.03	
2450896.8575	21.81 0.02	22.15 0.02	21.55 0.02	21.16 0.01	22.65 0.03	21.68 0.02	22.27 0.02	22.05 0.02	
2450932.7955	21.84 0.02	22.01 0.03	21.51 0.02	21.28 0.02	22.21 0.04	21.72 0.02	22.24 0.03	21.88 0.02	

Table 4—Continued

<hr/>									
<hr/>									
2450936.9023	21.92 0.04	22.00 0.04	21.53 0.03	21.46 0.03	22.17 0.05	21.67 0.03	22.27 0.05	21.86 0.04	
2450965.7179	21.95 0.04	21.66 0.02	21.40 0.02	21.75 0.03	22.12 0.07	21.68 0.03	22.49 0.05	21.77 0.02	
2450987.6717	22.02 0.04	21.53 0.01	21.39 0.02	22.23 0.03	22.30 0.03	21.66 0.02	22.70 0.05	21.85 0.02	
2450991.6879	21.97 0.02	21.48 0.01	21.33 0.02	22.24 0.03	22.27 0.02	21.65 0.01	22.59 0.03	21.78 0.01	
2450996.6918	21.99 0.04	21.39 0.02	21.23 0.02	22.30 0.06	22.28 0.05	21.65 0.03	22.58 0.06	21.85 0.04	
2451142.0300	21.66 0.02	21.63 0.02	21.80 0.03	21.50 0.02	22.41 0.03	22.05 0.02	22.67 0.04	22.27 0.03	
2451171.9956	21.42 0.01	21.80 0.02	21.94 0.03	21.92 0.03	22.70 0.05	22.20 0.03	22.75 0.05	22.36 0.03	
2451192.0452	21.38 0.01	21.80 0.01	21.89 0.02	22.08 0.02	22.58 0.03	22.18 0.02	22.63 0.03	22.40 0.02	
<i>g</i>									
2448622.9572	23.85 0.24	23.57 0.17	22.66 0.09	...	23.35 0.15
2449064.8359
2449076.8680	22.98 0.11	23.09 0.07	23.46 0.10	22.80 0.08	...	23.20 0.09
2450837.0286	23.38 0.09	23.43 0.07	23.05 0.05	23.01 0.05	24.01 0.12	...	24.09 0.13	23.51 0.08	
<i>i</i>									
2449417.8790	20.97 0.05	20.84 0.05	20.80 0.05	21.35 0.05	21.65 0.05	21.61 0.05	21.86 0.06	21.22 0.06	
2450226.6444	20.94 0.05	20.75 0.05	21.05 0.05	21.34 0.05	21.97 0.05	21.05 0.05	21.83 0.07	21.05 0.05	
<hr/>									
HJD	V33	V34	V35	V36	V37				
<i>r</i>									
2448269.9406	21.16 0.05	21.11 0.02	21.67 0.03	21.23 0.03			
2448359.7523	
2448388.7788	
<hr/>									
HJD	V33	V34	V35	V36	V37				
<i>r</i>									
2448622.9552	21.12 0.02	21.52 0.03	20.98 0.01	21.76 0.04	23.22 0.12				
2449064.8339	21.50 0.04	21.45 0.03	21.14 0.02	21.49 0.03	22.18 0.06				
2449421.8408	21.98 0.02	
2449427.8788	21.92 0.04	21.86 0.03	21.44 0.02	21.80 0.03	21.47 0.02				
2450189.8905	21.94 0.06	
2450190.9141	21.84 0.04	21.28 0.02	21.42 0.02	21.83 0.03	
2450191.7105	21.80 0.02	21.27 0.01	21.34 0.01	21.75 0.02	21.36 0.02				
2450192.7317	21.76 0.04	21.33 0.02	21.34 0.02	21.82 0.03	21.39 0.02				
2450213.8314	21.56 0.04	21.33 0.03	21.35 0.02	...	21.49 0.02				
2450216.8806	21.55 0.02	21.38 0.02	21.35 0.02	21.85 0.03	21.48 0.03				
2450226.6969	21.41 0.02	21.32 0.02	21.30 0.02	21.73 0.04	
2450489.9295	21.18 0.02	21.15 0.02	21.50 0.02	21.40 0.02	22.45 0.05				
2450509.7780	21.27 0.01	21.21 0.01	21.51 0.02	21.41 0.02	
2450510.9513	21.17 0.01	21.11 0.01	21.38 0.01	21.28 0.01	22.09 0.03				
2450511.7910	21.30 0.01	21.23 0.02	21.50 0.02	21.42 0.02	22.27 0.04				
2450834.0550	20.86 0.01	21.65 0.02	21.14 0.02	21.55 0.02	21.73 0.03				
2450835.9316	20.80 0.01	21.59 0.03	21.06 0.01	21.55 0.03	21.55 0.02				
2450837.0266	21.76 0.02	
2450867.9278	20.89 0.01	21.77 0.02	21.18 0.01	21.39 0.02	22.03 0.03				
2450870.9631	20.83 0.01	21.71 0.02	21.14 0.01	21.31 0.02	21.95 0.02				
2450872.9496	20.90 0.01	21.80 0.02	21.20 0.01	21.38 0.01	22.12 0.03				
2450873.9432	20.90 0.01	21.80 0.02	21.18 0.01	21.34 0.02	22.10 0.03				

Table 4—Continued

2450875.9306	20.88 0.01	21.72 0.01	21.15 0.01	21.30 0.01	22.07 0.02	
2450889.9782	20.93 0.01	21.68 0.03	21.19 0.02	21.23 0.02	22.32 0.06	
2450894.7555	20.93 0.01	21.72 0.02	21.22 0.02	21.24 0.02	22.28 0.04	
2450896.8575	20.93 0.01	21.66 0.01	21.22 0.01	21.24 0.01
2450932.7955	20.92 0.01	21.34 0.02	21.32 0.02	21.28 0.02	22.72 0.05	
2450936.9023	21.05 0.02	21.36 0.02	21.40 0.02	21.33 0.03	22.85 0.09	
2450965.7179	21.07 0.01	21.17 0.02	21.39 0.02	21.47 0.02	22.96 0.08	
2450987.6717	21.31 0.01	21.25 0.01	21.55 0.02	21.62 0.02
2450991.6879	21.25 0.01	21.19 0.01	21.48 0.01	21.53 0.01
2450996.6918	21.24 0.02	21.17 0.02	21.43 0.03	21.48 0.03
2451142.0300	22.14 0.04	21.81 0.03	21.51 0.02	21.31 0.01
2451171.9956	22.20 0.04	21.88 0.02	21.46 0.02	21.31 0.01
2451192.0452	22.22 0.02	21.78 0.01	21.42 0.01	21.21 0.01	21.77 0.02	
<i>g</i>						
2448622.9572	22.38 0.06	22.88 0.11	22.16 0.05	23.55 0.22
2449064.8359	22.91 0.12	...	22.39 0.07	23.01 0.17
2449076.8680	22.58 0.05	22.91 0.10	22.38 0.05	22.70 0.08	23.52 0.09	
2450837.0286	22.38 0.05	23.28 0.05	...	23.22 0.06	23.55 0.07	
<i>i</i>						
2449417.8790	20.83 0.05	20.80 0.05	20.50 0.05	20.76 0.05
2450226.6444	20.73 0.05	20.62 0.05	20.49 0.05	20.75 0.05

Table 5. Cepheid Variables

Object	Period	$\langle g \rangle^a$	$\sigma_{\langle g \rangle}$	$\langle r \rangle^b$	$\sigma_{\langle r \rangle}$	$\langle i \rangle^c$	$\sigma_{\langle i \rangle}$	X	Y	RA [J2000]	DEC[J2000]
	[days]										
C01	18.65	23.59	0.21	23.45	0.09	23.47	0.24	177.17	931.06	12:26:16.8	33:33:07
C02	12.99	24.24	0.26	23.84	0.11	23.44	0.23	477.19	143.28	12:26:12.9	33:30:33
C03	15.06	24.13	0.25	23.55	0.10	22.82	0.19	863.10	198.74	12:26:06.3	33:30:42
C04	71.26	21.60	0.08	21.35	0.02	21.23	0.16	870.34	152.16	12:26:06.3	33:30:33
C05	26.20	23.12	0.19	23.26	0.08	23.18	0.21	962.14	780.46	12:26:03.9	33:32:35
C06	25.80	23.33	0.19	23.16	0.08	22.91	0.18	1493.71	878.36	12:25:54.9	33:32:51
C07	27.99	22.70	0.30	22.81	0.06	22.86	0.22	1551.86	69.44	12:25:55.0	33:30:14
C08	12.09	24.62	0.29	24.11	0.17	1567.74	346.60	12:25:54.3	33:31:07
C09	57.80	22.90	0.05	22.32	0.04	22.24	0.16	1612.33	419.98	12:25:53.5	33:31:22
C10	52.90	22.73	0.13	22.28	0.04	22.30	0.17	1647.97	1365.20	12:25:51.6	33:34:25
C11	89.89	22.03	0.03	21.56	0.02	21.57	0.16	1810.24	1237.91	12:25:49.1	33:34:00

^aMean g as computed in equation 4

^bPhase-weighted intensity average

^cMean i from $r - i$ at i phase

Table 6. Other Variable Stars

Object	Period [days]	$<g>$ ^a	$<r>$ ^a	$<i>$ ^b	Δr ^c	X	Y	RA [J2000]	DEC[J2000]
V01	570.0 ^e	22.97	21.75	20.83	0.89	144.09	1154.40	12:26:17.1	33:33:51
V02	207.8	24.82	23.39	22.36	0.92	208.96	360.19	12:26:17.1	33:31:16
V03	211.0 ^e	22.48	21.37	20.54	1.32	216.63	202.95	12:26:17.1	33:30:46
V04	181.1	24.67	23.25	22.15	0.71	336.22	1638.35	12:26:13.2	33:35:24
V05	237.9 ^e	22.17	20.91	20.13	0.67	515.87	322.67	12:26:12.0	33:31:07
V06	818.9 ^e	22.84	21.70	20.94	1.13	651.49	536.32	12:26:09.4	33:31:48
V07	680.1	23.40	22.22	21.53	0.49	731.36	339.72	12:26:08.3	33:31:10
V08	505.3	23.03	21.60	20.90	0.48	953.77	282.99	12:26:04.7	33:30:58
V09	456.8	23.23	22.14	21.23	0.68	988.34	360.40	12:26:04.0	33:31:13
V10	305.7	22.86	21.95	21.33	0.42	1028.76	417.52	12:26:03.3	33:31:24
V11	821.8 ^e	23.45	22.09	21.17	0.70	1053.51	382.39	12:26:02.9	33:31:17
V12	1500.0 ^e	22.16	20.94	20.30	0.63	1139.67	617.67	12:26:01.1	33:32:02
V13	570.8	22.35	21.46	21.08	0.67	1179.05	503.46	12:26:00.6	33:31:40
V14	581.7	22.76	21.64	20.79	0.80	1236.18	637.74	12:25:59.5	33:32:06
V15	818.5	22.17	21.32	20.39	1.29	1278.18	287.68	12:25:59.3	33:30:57
V16	766.8 ^e	24.30	23.35	22.42	1.17	1309.85	168.09	12:25:58.9	33:30:34
V17	504.2 ^e	23.28	21.88	21.06	0.78	1348.81	10.17	12:25:58.5	33:30:03
V18	264.6	24.98	23.88	22.95	0.81	1361.41	1518.60	12:25:56.2	33:34:56
V19	1024.7 ^e	21.91	20.79	20.19	0.65	1406.63	49.68	12:25:57.4	33:30:10

Table 6—Continued

Object	Period [days]	$<g>$ ^a	$<r>$ ^a	$<i>$ ^b	Δr ^c	X	Y	RA [J2000]	DEC[J2000]
V20	411.4 ^e	22.27	21.23	20.52	0.60	1427.24	1590.98	12:25:55.0	33:35:10
V21	211.6 ^e	23.07	21.78	20.95	0.76	1432.33	721.64	12:25:56.1	33:32:21
V22	207.6 ^e	22.64	21.38	20.54	0.92	1447.10	436.87	12:25:56.2	33:31:26
V23	426.0 ^e	22.98	21.54	20.86	0.80	1459.51	452.04	12:25:56.0	33:31:28
V24	609.2	22.17	20.91	20.34	0.82	1462.68	326.57	12:25:56.1	33:31:04
V25	1014.7	23.16	21.66	21.11	0.59	1463.24	235.67	12:25:56.2	33:30:46
V26	450.3 ^e	23.28	21.74	20.80	0.78	1565.12	473.45	12:25:54.2	33:31:32
V27	509.7 ^e	23.04	21.68	20.48	0.93	1589.24	304.76	12:25:54.0	33:30:59
V28	184.6	23.01	21.65	21.49	1.09	1599.61	261.24	12:25:53.9	33:30:51
V29	333.2	23.67	22.37	21.68	0.64	1615.12	945.73	12:25:52.7	33:33:04
V30	447.7	22.73	21.80	21.25	0.84	1621.51	750.46	12:25:52.9	33:32:26
V31	537.9	24.09	22.62	21.74	0.57	1689.84	1262.81	12:25:51.1	33:34:05
V32	443.7	23.34	22.04	21.11	0.57	1706.81	705.39	12:25:51.5	33:32:17
V33	545.2 ^e	22.57	21.37	20.50	1.41	1790.41	1396.61	12:25:49.2	33:34:31
V34	246.2	22.92	21.49	20.63	0.77	1806.01	1176.02	12:25:49.2	33:33:48
V35	555.7	22.27	21.34	20.48	0.51	1823.23	651.81	12:25:49.7	33:32:06
V36	413.5	23.19	21.48	20.45	0.56	1831.45	931.76	12:25:49.1	33:33:00
V37	604.8	23.53	21.91	...	1.75	2007.94	1209.67	12:25:45.8	33:33:53

^aPhase-weighted intensity average^bMean i from $r - i$ at i phase^c $\Delta r = r$ peak to peak amplitude^ePeriod uncertain

Table 7. Individual distance moduli and reddening values of Cepheids in NGC 4395 using g and r magnitudes.

ID	PL-relation with trans. by Kent ^a				PL-relation with synthetic trans. ^b			
	μ_g	μ_r	$E(g-r)$	μ_0	μ_g	μ_r	$E(g-r)$	μ_0
C01	28.375	28.278	0.097	28.040	28.298	28.339	-0.041	28.438
C02	28.620	28.213	0.407	27.219	28.541	28.267	0.273	27.600
C03	28.672	28.107	0.565	26.727	28.594	28.164	0.430	27.114
C04	27.913	27.871	0.042	27.769	27.841	27.955	-0.114	28.233
C05	28.293	28.518	-0.225	29.068	28.217	28.585	-0.368	29.483
C06	28.491	28.393	0.099	28.152	28.416	28.459	-0.044	28.566
C07	27.951	28.146	-0.195	28.621	27.876	28.214	-0.338	29.039
C08	28.917	28.387	0.530	27.093	28.838	28.440	0.398	27.470
C09	28.975	28.580	0.395	27.616	28.903	28.661	0.242	28.070
C10	28.703	28.421	0.282	27.733	28.631	28.500	0.130	28.182
C11	28.609	28.370	0.239	27.786	28.539	28.459	0.081	28.261
Mean:	28.502	28.299	0.203	27.802	28.427	28.367	0.059	28.223
	± 0.104	± 0.061	± 0.081	± 0.202	± 0.104	± 0.062	± 0.081	± 0.205

^aPL-relation of Madore & Freedman (1991) with transformations by Kent (1985).

^bPL-relation of Madore & Freedman (1991) with synthetic transformations.

Table 8. Individual distance moduli and reddening values of Cepheids in NGC 4395 using r and i magnitudes.

ID	PL-relation with trans. by Kent ^a				PL-relation with synthetic trans. ^b			
	μ_r	μ_i	$E(r-i)$	μ_0	μ_r	μ_i	$E(r-i)$	μ_0
C01	28.278	28.342	-0.064	28.517	28.339	28.381	-0.042	28.497
C02	28.213	27.841	0.372	26.830	28.267	27.869	0.398	26.785
C03	28.107	27.414	0.693	25.529	28.164	27.446	0.718	25.494
C04	27.871	27.849	0.022	27.788	27.955	27.928	0.027	27.856
C05	28.518	28.495	0.023	28.431	28.585	28.544	0.041	28.433
C06	28.393	28.205	0.188	27.694	28.459	28.254	0.206	27.694
C07	28.146	28.261	-0.115	28.574	28.214	28.312	-0.099	28.581
C08	28.387	28.440
C09	28.580	28.586	-0.006	28.601	28.661	28.659	0.002	28.655
C10	28.421	28.530	-0.109	28.827	28.500	28.601	-0.101	28.875
C11	28.370	28.491	-0.121	28.820	28.459	28.578	-0.119	28.903
Mean:	28.299	28.201	0.088	27.961	28.367	28.257	0.103	27.977
	± 0.061	± 0.121	± 0.083	± 0.335	± 0.062	± 0.125	± 0.085	± 0.344

^aPL-relation of Madore & Freedman (1991) with transformations by Kent (1985).

^bPL-relation of Madore & Freedman (1991) with synthetic transformations.